Redesign of the Cinnamon Production Line to Reduce its Total Loss by 5%.

Master's Design Project

Industrial Engineering and Management
Smart Systems in Control and Automation

In collaboration with:

Author:
Thomas Ike
s2252236

Supervisors:
dr. J. Vos
prof. dr. A. Vakis

October 2018

Abstract

Ever since the Indonesian based spices company Tripper Nature established its large-scale cinnamon grinding facility in Jakarta, they have coped with an average production loss of 7.43% for their most popular cinnamon product: DRAG60. This research aimed at reducing the production loss, occurring in grinder GRIN01, by identifying and implementing a proper solution. Initial investigation on the true cause of the production loss showed that high temperatures of 57.2°C during the grinding process, cause the moisture and volatile oil in the cinnamon to evaporate, decreasing their weight based content which results in direct weight loss of the output. Through a theoretical analysis of the complete dynamics, the main contributing factors to the high temperatures were identified that enabled us to propose three candidate solution for further analysis. Upon conducting experiments on these solutions and analysing the results, the most suitable solution that arose, was to optimise the settings for the grinder in combination with the installation of an external inlet cooling system onto it. After implementation of the solution and verifying the expected results of the measure through large-scale production, we were able to achieve a loss reduction of 5.14% for DRAG60 with an additional loss reduction of 3.10% for DRAG50 (a different cinnamon product, also processed by GRIN01). The expected yearly savings that follow this loss reduction is equal to $321,881.

Contents

1 Introduction

This Design Project is the result of an eighteen-week internship to conclude the final stage of the two year Master programme in Industrial Engineering and Management. The internship takes place at an Indonesian based spices company called PT. Tripper Nature, Jakarta. In total, they produce nine different spices, of which cinnamon is one of their main products. Ever since the large-scale production of cinnamon started in 2014, they have coped with an average production loss of 7.43%, which they have not been able to resolve as of yet. This Design Project aims at finding the cause of this production loss and will propose and implement a redesign of the cinnamon production line to reduce it.

1.1 PT. Tripper Nature

PT. Tripper Nature was founded in 1992 by the two French brothers Francois an Olivier Bernard who grew up in Sumatra, Indonesia. In the mid-80s, Francois lived in Los Angeles but frequently helped his father collecting vanilla beans in Bali. It was during this activity, that he saw the business opportunity to sell vanilla beans to restaurant owners in LA. He seized the opportunity with his brother and due to their history with Indonesia, the company started to grow quickly in the following years.

In 2001, Tripper Nature started to process cinnamon in a dedicated milling plant in Jakarta, followed by an extraction facility in Bali in 2004. After moving back and forth the milling plant between Jakarta and Bali, they eventually decided to base the large-scale production facility in Jakarta in 2014. Nowadays, the plant in Jakarta processes cinnamon, turmeric and ginger. Most other spices are still processed in Bali's plant.

1.2 Cinnamon

Cinnamon is part of the *Cinnamomum* genus which is an aromatic tree type belonging to the *Lauraceae* family. Cinnamon comes from stripping the bark of the cinnamon tree and letting it dry, such that is rolls into cinnamon bars of different sizes. Original cinnamon is native to Sri Lanka, also known as Ceylon cinnamon, while Cassia cinnamon is native to China and Indonesia. Although they both belong to the Cinnamomum genus, their difference lies in the taste which differs per country. Generally speaking, Ceylon cinnamon has a milder taste, sweeter flavour and is more expensive compared to Cassia cinnamon.

This research focuses on the processing of Cassia cinnamon from Indonesia, also known as Indonesian cinnamon. It is the dried bark of the *C. burmannii* tree, mainly grown in West Sumatra with an area of around 29,000 ha (Ravindran et al., 2003).

2 System Context: Cinnamon Tree to Cinnamon Powder

This chapter creates an overview of the whole production system to determine the scope of the project. We start by giving a short description of the supply chain, followed by the cinnamon grinding process and the different product types.

2.1 Cinnamon Supply Chain

The cinnamon supply chain starts at a tree plantation in West Sumatra, where the trees grow to sufficient size for harvesting. After harvesting the cinnamon bark and drying it, they store the cinnamon bars in the warehouse before shipping it to Jakarta or Bali. Tripper Nature processes the cinnamon bars by grinding, extracting, distilling or spray drying. The Jakarta facility focuses on grinding only, hence the other processes will not be discussed further in this research. For a more elaborate supply chain description, see Appendix A.

2.2 Cinnamon Grinding Process

As depicted in Figure 2.1, the production of cinnamon ground can be divided into two main steps. The first step transforms the raw material (cinnamon bars) into so-called work-in-progress or WIP material. This step consists of putting the cinnamon bars on the conveyor belt for manual sorting, to filter out any non-cinnamon products such as plastics, stones, and metals. At the end of the conveyor belt, the cinnamon bars fall into the shredder (GRIN03) to be reduced to the desired average WIP size of 20 mm. To ensure that the average size of the cinnamon corresponds to the desired size, a sifting process is present. In this process, two big shaking sieves operate above each other, letting the desired size of cinnamon pass trough while any material that is too big will be transported back onto the conveyor belt to be shred again. Furthermore, each sifting machine has an additional air sorting machine after the sieve, which blows light material upwards, while the (heavier) cinnamon falls to the next step. After the cinnamon passes the 20 mm sieve and a metal detector, it falls into a jumbo bag and is labelled as WIP material. This jumbo bag is then transported into the WIP warehouse.

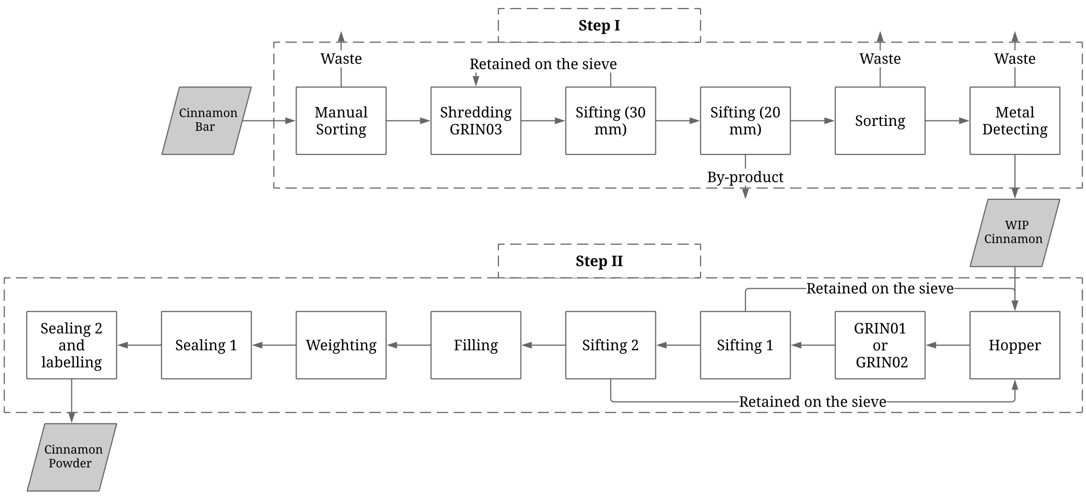

Figure 2.1: Cinnamon Production Line Schematic.

The second step of the process reduces the WIP material into different sizes by loading it into the hopper, which feeds the WIP material to the grinder at a constant speed. The ground cinnamon from a grinder (GRIN01 or GRIN02) moves to two sieves which let the desired particle size pass while transporting the bigger particles into jumbo bags as by-product for later use. After reaching the desired particle size, the cinnamon falls to the filling station below, into a plastic bag until reaching the desired weight. Afterwards, the plastic bag is sealed, boxed and labelled with the corresponding product code.

2.3 Product Types

Tripper Nature reduces the WIP material into three types of grinds: cut, tea bag cut (TBC) and powder. Each product type has a product code: DRAGxx. DRAG comes from the brand name Dragon Cinnamon, and the xx denotes the granulation specification in the Standard US Mesh size but does not correspond to the average size. The Standard US Mesh is used to indicate the particle size of a product by checking whether it passes through a sieve with a specific mesh. The US Mesh number represents how fine the sieve is, meaning that a 100 US Mesh sieve has openings of only 0.149 mm, while a 10 US Mesh sieve has openings of 2 mm. This way, sieves can be used to ensure that the ground cinnamon is of the desired granulation (Saravacos et al., 2002).

Table 1 shows all the different product types, from coarse to fine granulation. The broken cinnamon (DRAG02) is the WIP material coming from the shredder (GRIN03). The other three product types (cut, TBC and powder) are produced using the two available grinders in the plant: GRIN01 and GRIN02. GRIN01 is in use for large-scale fine grinding and GRIN02 for small-scale production and coarse grinding.

Table 1: Product types and mesh sizes.

Grinder	Product type	Product code	Granulation specification		
GRIN03	WIP (Broken)	DRAG02	>90%	+2	US Mesh
GRIN02	Cut	DRAG06	>95%	+10	US Mesh
	Tea bag cut	DRAG10	>75%	+10	US Mesh
	Tea bag cut	DRAG18	>85%	-10 +35	US Mesh
GRIN01	Powder	DRAG50	<5%	+48	US Mesh
			10-20%	-48 +60	US Mesh
			25-40%	-60 +100	US Mesh
			<60%	-100	US Mesh
	Powder	DRAG60	100%	-30	US Mesh
			>95%	-60	US Mesh
			>70%	-100	US Mesh

The US Mesh sizes in the table represent the requirements for sample testing of the ground cinnamon. For example, of adequately produced DRAG60, 70% should pass the 100 US Mesh sieve, 95% should pass the 60 US Mesh sieve and 100% should pass the 30 US Mesh sieve. Furthermore, a plus sign indicates that it should not pass the sieve.

3 Problem Analysis

This chapter uses the previously described system context to further scope the research towards the problem. The problem description is based on field observations, old data and talks with employees at Tripper Nature. After the problem definition, we construct a proper research goal and accompanying research questions.

3.1 Problem Owner

The problem owner for this project is Albert Putra, who is the cinnamon business manager of Tripper Nature. He is responsible for the production of cinnamon and is part of Tripper Nature's management team.

3.2 Problem Description: Evaporation as the Culprit of Loss

During conversations with the cinnamon business manager and the head of operations, they mentioned an interesting relation between the loss for different products and their accompanying grinding temperatures. They stated that the higher the grinding temperatures, the higher the loss.

To check this claim, Table 2 shows the average loss and temperature per product type, based on data analysis from September 2014 until May 2018. A found correlation coefficient of 0.87 between the five data points for the loss and temperature indeed indicates a strong relationship, however, it gives us no information on the causality of the relationship. Furthermore, making a comparison between GRIN02 and GRIN01 should be done with some discretion because of different grinding dynamics (capacity, size, mill type, number of plates etc.). Nonetheless, the same observation can be made independently for both grinders: higher temperatures accompany higher loss.

Table 2: Average (weight) loss of products in GRIN01 and GRIN02 and their temperatures.

	GRIN01		GRIN02		
	DRAG60$_{N=823}$	DRAG50$_{N=97}$	DRAG18$_{N=145}$	DRAG10$_{N=41}$	DRAG06$_{N=36}$
Loss (%)	7.43	4.46	1.84	1.65	0.95
T_{grin}(°C)	57.2	38	41.0	38.4	33.7

Since the loss and temperature for DRAG60 are paramount, the focus of this research will mainly be on GRIN01 and its loss during the production of DRAG60. However, the possible solution to reduce the loss might also be applicable for DRAG50.

3.2.1 Causality between loss and temperature

As mentioned, the found correlation coefficient of 0.87 between the loss and the temperature shows a strong relationship but does not necessarily indicate a causal relationship as well. Through field observations and literature research, a total of three causes are identified that can explain the occurrence of loss. Two of which indicate a causal relationship between the grinding temperature and the loss, while the third explains the existence of loss in general.

The first finding was the presence of an oily substance in the machines and piping after the grinder, shown in Figure 3.1. The Quality Control (QC) department tested this substance and concluded that it consists of water and cinnamon oil, origination from the cinnamon itself. The presence of the oily substance in the machines and piping indicates the occurrence of an evaporation-condensation effect, taking place in the grinder and machines afterwards. This effect is also discussed by Singh and Goswami (1999); Murthy and Bhattacharya (2008); Barnwal et al. (2014a). In our case, the evaporation effect starts in the grinder due to the previously found high grinding temperatures that cause the moisture and volatile oil in the cinnamon to evaporate. When the evaporated oil and water exits the grinder, the condensation effect of both substances starts because of the relative temperature decrease in the machines and piping after the grinder. The inevitable effect of evaporation of these substances on the loss is that it decreases their weight based content in the cinnamon, resulting in overall weight loss of the material. Furthermore, the decrease of volatile oil in any spice results in loss of taste and smell, hence the evaporation also results in a slight decrease in product quality (Ravindran et al., 2003).

Figure 3.1: Oily substance found in the product collector and cinnamon sticking in piping after the grinder.

The second finding was that inside the piping after the grinder, a thick layer of (blackened) cinnamon is present, shown in Figure 3.1. This layer is the results of cinnamon passing the condensed (dark) oily substance, causing it to stick to it. This process is repeated over and over for every production batch, resulting in the buildup of the cinnamon layer over time. The sticking cinnamon in the piping reduces the total output and thus increases the loss as well. Furthermore, it requires periodic cleaning of the piping and machines, creating production downtime.

The last finding was that the WIP material in the relatively warm warehouse loses weight during the period it is stored, expectantly due to slow evaporation of moisture and volatile oil as well. Since Tripper Nature registers the losses from Table 2 by measuring the difference in weight directly after GRIN03 and GRIN01, the losses include both the loss induced by the grinding temperatures and the general warehouse loss.

Figure 3.2 shows the summary of the findings, and indicates the causal relationship between the grinding temperature and the loss.

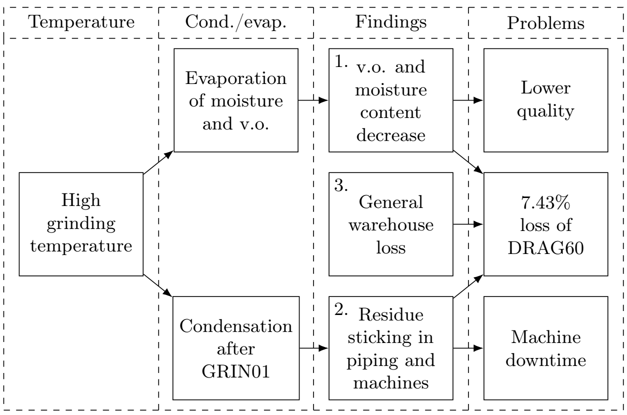

Figure 3.2: Visualisation of the three findings, to show the causal relationship between high temperatures and loss (⟶ 'results in').

3.2.2 Contribution of findings to the loss

The average registered loss of DRAG60 can be attributed to three possible factors; evaporation of moisture and volatile oil during production, residue sticking in the piping and general warehouse loss. It is therefore important to determine the contribution to the loss for each of them, to further scope the problem definition. The contribution of sticking residue is hard to estimate since no data is available on the quantities, but, the impact is expected to be minimal. However, we are able to determine the contribution of the evaporation effect in the grinder, since the moisture and volatile oil content of all the products have been monitored since 2014 for the sake of quality control. Furthermore, the warehouse loss has been monitored by the production manager with an average of 1.2%. Based on this data, the contribution of the evaporation effect in the grinder and the warehouse to the total loss can be estimated. Table 3 shows the averages for the moisture and volatile oil content of the WIP input material, DRAG60 and DRAG50 (for comparison).

Table 3: The average moisture and volatile oil content, before and after grinding.

	$\text{WIP}_{N=145}$	$\text{DRAG60}_{N=823}$	$\text{DRAG50}_{N=145}$
Moisture (% d.b.)	14.54	9.87	12.34
Volatile Oil (% w.b.)	3.52	3.06	3.28

According to Ullmann et al. (1985) the density of moisture and volatile oils is approximately one, where the oil is slightly less dense. Using this information, the decrease in moisture and volatile oil content denoted in Table 3 can be used directly to estimate their contribution to the weight loss by

$$L_{M,V} = (C_i - C_f(1 - L)) \cdot 100\%. \tag{3.1}$$

Here $L_{M,V}$ represents the loss caused by the evaporation of moisture (M) or volatile oil (V), calculated using their initial and final contents (C_i, C_f) and the total loss L. The results from this calculation in Figure 3.3 show that the moisture and volatile oil loss during the grinding process are the main contributors, in addition to the warehouse and residue loss. For DRAG60, the loss induced by the grinder adds up to 6.23%, which is equal to 84% of the total loss. The lower contribution of volatile oil evaporation compared to moisture is because of its higher boiling point that reduces its tendency to evaporate (Ullmann et al., 1985). Please note that these values are all based on averages over the past years, in reality, they can differ per season.

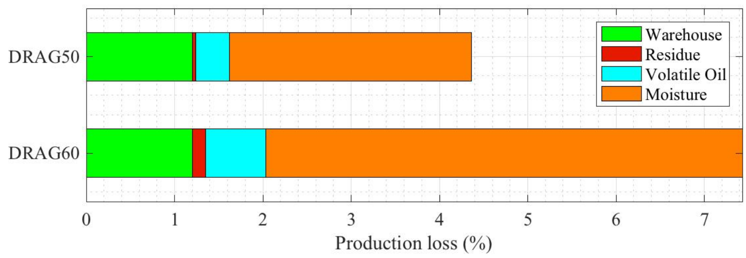

Figure 3.3: Contribution of the four found factors to the loss.

To conclude on the results for the contribution calculation, the evaporation of moisture and volatile oil during the grinding process appears to be the culprit of the production loss, in addition to the warehouse loss. Furthermore, the high temperatures in the grinder result in a side effect of creating residue in the piping and a decrease in product quality.

Therefore, the problem statement becomes:

> *The evaporation effect due to high temperatures in GRIN01 causes an unwanted loss of 6.23%, residue forming after the grinder and a decrease in final product quality.*

3.3 Research Scope: Pulverising Machine GRIN01

Based on the above-described problem, the research scope becomes grinder GRIN01 and its high temperatures during the production of DRAG60. The installed grinder at Tripper Nature is the Air Swept Pulveriser (ASP) Model 28-H, manufactured by Reynolds Engineering & Equipment. This pulveriser does not grind in the 'traditional' way, by crushing material between two surfaces to the desired size. Instead, it reduces the size of material by impacting the material at very high speeds, as will be discussed below.

3.3.1 Complete pulverising system

The complete pulverising system in Figure 3.4 consists of four main parts: the *feeder*, the *pulveriser (grinder)*, the *product collector* and the *exhaust fan*.

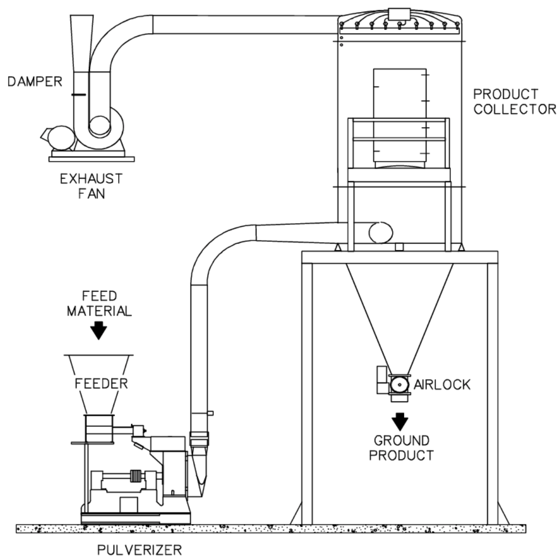

Figure 3.4: The complete pulverising system (Reynolds Engineering & Equipment, 2001).

The process starts at the feeder (hopper) which feeds the to-be-ground material (WIP) into the pulveriser (grinder) at a constant speed. Once it falls into the pulveriser, impact breaks down the cinnamon, and the decreased (lighter) particles are sucked out by the exhaust fan due to a created vacuum. The air stream leads the ground cinnamon into the product collector, where the cinnamon falls into the cone due to the sudden pressure difference. The lighter material will still be sucked up but is caught by very fine cylindrical dust collectors in the top of the product collector shown in Appendix B. To release the dust from the cylindrical dust collectors, a pneumatic pulse is given at specific intervals. After production, the airlock opens such that the ground product can be transported to the sifting tower (outside the scope of this research).

The described evaporation effect of moisture and volatile oil occurs inside the pulveriser grinding chamber and then condensates in the pipe after the grinder, the product collector (Figure 3.1) and exhaust fan. The amount of moisture and volatile oil that condensates happens to such an extent that one can see it dripping out of the exhaust pipe. Due to this condensation, the cylindrical dust collectors are cleaned every month and replaced every three months.

3.3.2 The pulveriser: GRIN01

Figure 3.5, shows the cross-section of the pulveriser (GRIN01) where on the top left the WIP cinnamon is fed into the grinder by the feeder, and on the top right, the fine cinnamon powder is sucked out by the exhaust fan. The particle size reduces by impacting the WIP particles with beater plates, equipped with fixed beaters (B), rotating at very high speeds within close proximity to the wear liners (A). These parts are designed to provide maximum turbulence in the grinding zone. After being hit by the beater plates, the particles are thrown against the corrugated wear liners, causing size reduction. The particles bounce off the liners and are hit by the beater plates again. This effect occurs over and over again, causing particle size and density reduction until the centrifugal force imparted by the rotating beater plates is overcome by the air stream passing through the pulveriser. At this time, the smaller particles are pulled from the pulveriser by the air stream and transported to the product collector (Reynolds Engineering & Equipment, 2001).

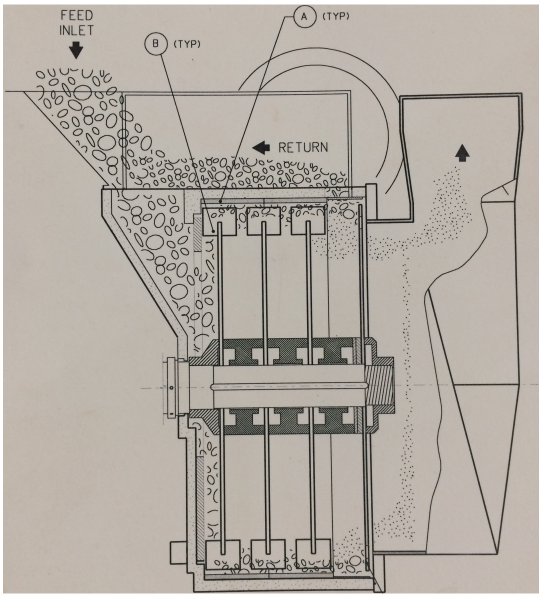

Figure 3.5: Cross section GRIN01(Reynolds Engineering & Equipment, 2001).

Figure 3.6: Inside GRIN01, showing the beater plate with beaters close to the lining.

For different cinnamon products, a total of five controlled parameters can be identified than can be preset before production. Table 4 shows these parameters, their ranges and the settings for DRAG60 and DRAG50.

Table 4: Controlled parameters and the current settings.

Parameter	Unit	Ranges	DRAG60	DRAG50
Beater rotating speed	RPM	0 - 1750	1650	950
Feeder speed	RPM	25 - 45	40	33
Number of blades	#	1 - 3	3	3
Input size	US Mesh	2 - 60	2	2
Output size	US Mesh	50 - 250	200	110

3.4 Stakeholders and Requirements

According to Freeman (2010), a stakeholder is defined as:

> "A stakeholder is any group or individual who can affect or is affected by the achievement of the organisation's objective."

Based on the described problem and its system description, the relevant stakeholders for this research can be identified together with their requirements.

Cinnamon business manager (Albert)
Albert is the cinnamon business manager who is part of the board of directors at Tripper Nature. He is responsible for the performance of the production line and has a high interest in reducing the production loss. Preferably, he would like the loss for DRAG60 to be similar (or a bit higher) to the losses that occur in GRIN02. Therefore he set the desired loss reduction to be about 5%. Furthermore, he stated that capital and operational expenditures for a solution can be made, but only under the condition that the resulting savings will be significant with respect to the involved costs. In addition, since the DRAG60 from Tripper Nature is an A-grade product on the market, the quality requirements are stringent concerning minimal granulation, volatile oil content and moisture content.

Production manager (Madhy)
Madhy is head of operations who is responsible for the production planning in the whole factory and registers all production in the databases. He is well aware of the production loss and also has a high interest in resolving the issue. Since Madhy is responsible for the production planning, he can arrange experimental setups in the planning and also register the results. His main requirements for the possible solution are that it should be feasible in terms of this planning and that the average production rate for DRAG60 is met.

Production engineer (Paryanto)
Paryanto is the production engineer and has the technical knowledge regarding the grinder. He has the practical know-how on the settings and limitations of the machines and their effects on the output. He will be involved during experiments with solutions and oversees the implementation process.

Operators
During production at GRIN01, four operators take care of the input and output and monitor the grinder. During the research, their contribution is mainly by monitoring different parameters during production. Furthermore, they can be affected by possible changes in the grinder setup as a result of this research.

Table 5 lists the requirements and possible restrictions to the research that are identified by the stakeholders.

Table 5: Stakeholder requirements.

Stakeholder	Requirement for solutions	Quantification
Cinnamon business manager	Reduce the production loss for DRAG60	-5%
	Meet granulation specifications	Table 1
	Minimum volatile oil content	2.5%
	Minimum moisture content	7.5%
	Financial feasibility	-
Production manager	Experiments cannot interfere with production	-
	Planning feasibility	-
	Average production rate of DRAG60	$\geq$800 kg/h
Production engineer	Parameter settings should stay within range	Table 4
	Implementation feasibility	-
Operators	-	-

3.5 Research & Design Goal

The research and design goals aim to solve the issue of loss due to the evaporation of moisture and volatile oil. The research goal is formulated around identifying different ways of minimising the evaporation effect and the design goal aims at the eventual design and implementation of the best solution.

The research goal therefore becomes:

> *To identify ways of minimising the evaporation loss of 6.23% as to reduce the total production loss for DRAG60 by 5%.*

So the design goal becomes:

> *To design and implement the most suitable solution in or on the grinder and determine the optimal machine settings.*

The addition of the determination of new parameter settings to the design goal is because of the expectancy that the dynamics of the grinding process will change after implementing the solution.

3.6 Research Question

With the problem defined in Section 3.2 and its accompanying goal in Section 3.5, the research questions can be constructed. The main research question is:

> *What is the best way to minimise the evaporation effect in GRIN01 to reduce the total production loss by 5% and how does it perform?*

The accompanying sub-questions are:

SQ1 *What are the causes of the high grinding temperatures that result in the evaporation effect?*

SQ2 *What are candidate solutions for reducing the evaporation effect in the grinder?*

SQ3 *What is the best way to reduce the loss due to evaporation?*

SQ4 *How should the solution be implemented?*

SQ5 *What are the new parameter settings that meet all the stakeholder requirements?*

SQ6 *What is the eventual loss reduction as a result of the new measure and its settings?*

In Section 4 the complete research design is discussed to answer the research question and sub-questions.

4 Research Design

This chapter discusses the created research design around the research questions to reach the eventual goal of 5% loss reduction. First, it is determined whether the research is practice or knowledge oriented. Afterwards, a decision is made on the appropriate choice of a cycle for this research. Finally, a description of tools and methods will be provided per sub-question together with an overall project planning.

4.1 Research Orientation

As for the research orientation, there exists a distinction between practice-oriented research (POR) and knowledge oriented research (KOR). Practice-oriented research tries to find practical solutions to problems, whereas knowledge oriented research has the purpose of adding findings to the knowledge base. In addition to the orientation of the research, there are two main approaches to conduct the research: either deterministic or holistic. A deterministic approach is also called causal determinism where everything is explained based on cause-and-effect relations. A holistic approach, on the contrary, looks at systems as a whole, where elements are best understood in relations to each other and the total system.

Based on the defined problem and goal for this research, one can conclude that it is mainly practice-oriented in combination with a deterministic approach. There is a specifically formulated problem with a clear goal, which demands a practical solution regarding the minimisation of the evaporation effect. This eventual solution will probably only be relevant for Tripper Nature and does not contribute to the knowledge base in a more general sense. Furthermore, the approach to finding adequate possibilities will be deterministic, since the research aims at finding possible ways to reduce the loss and determine their impact, hence a cause-and-effect analysis. Figure 4.1 gives a graphical representation of the research orientation.

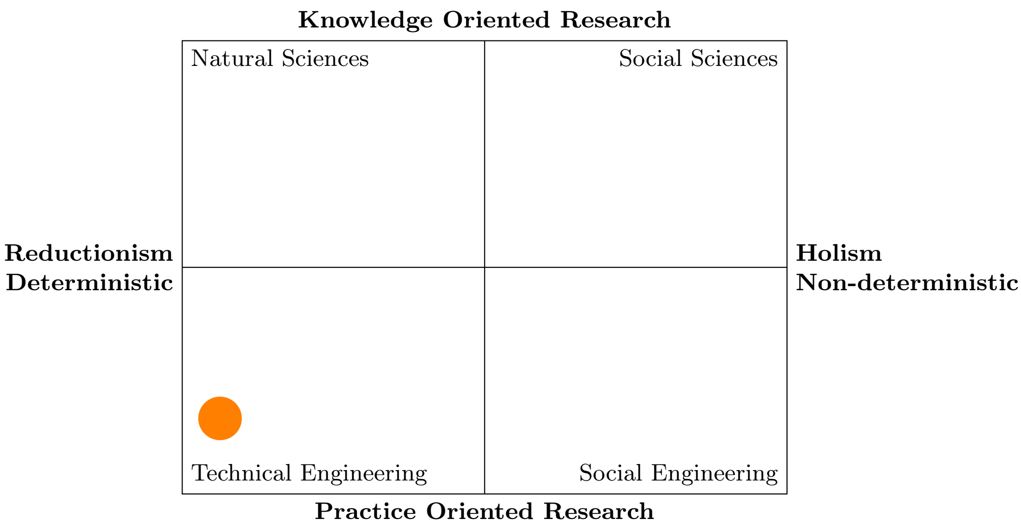

Figure 4.1: Research orientation and approach of this Design Project.

4.2 Choice of Cycle

Based on the research orientation and the defined problem and goal in mind, the three cycle view of Hevner would be the most suitable cycle to pick (Hevner, 2007). This cycle enables a researcher to link the environmental requirements together with foundations in the knowledge base, to eventually design the solution. Below, a more elaborate description per cycle is given:

- **The Relevance Cycle**: A proper design research starts by identifying all requirements that are relevant for the defined problem. Since these requirements have a direct impact on the eventual design of the solution, the relevance cycle is crucial in the initial steps of the research. Section 2 & Section 3.2 focused on getting to know the application domain by talking to relevant people, get to know the technical system and be able to conclude on a proper problem description. Furthermore, the relevance cycle will be used throughout the whole research, since it also enables evaluation of proposed solutions and possible changes to the requirements.
- **The Rigor Cycle**: The rigor cycle is used to relate past knowledge to the research through scientific theories and expertise, but also by looking at comparable applications of existing artefacts in the application domain. Although they are not directly applicable to the current problem of Tripper Nature, they can give great insight into possible ways of reducing loss. Furthermore, the knowledge base will be used to find literature related to grinding and to confirm certain finding from the field testing in the relevance cycle.
- **The Design Cycle**: This cycle aims at building a new artefact that will resolve the issue of production loss, by constantly iterating between the relevance cycle and the rigor cycle. This two-way working principle also enables the researcher to constantly evaluate the artefact through the use of literature in the rigor cycle and hands-on results from field testing in the relevance cycle.

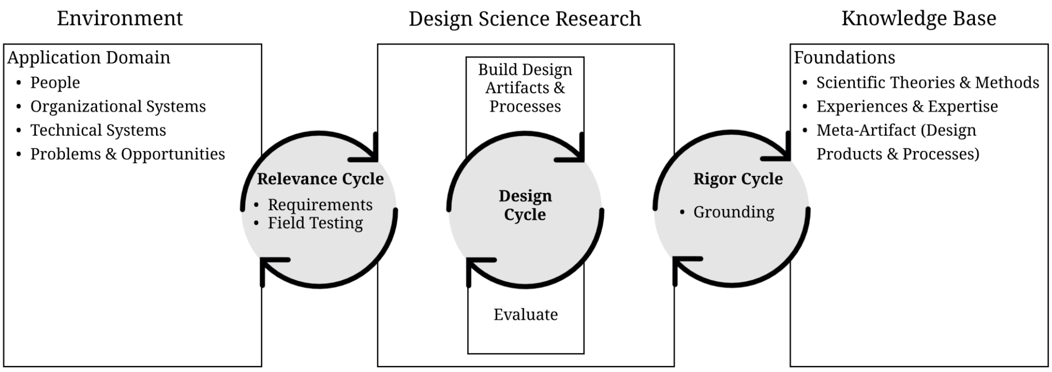

Figure 4.2: Three Cycle View on Design Cycle Research.

4.3 Research Tools, Methods and Structure

Various methods and tools will be used throughout this research to answer the research question and sub-questions. Therefore, an elaboration is given on every sub-question by first describing its (sub) goal, together with the methods used to achieve the goal.

SQ1 *What are the causes of the high grinding temperatures that result in the evaporation effect?*

Here the dynamics of the grinding process will be determined by a cause-and-effect analysis, extending the diagram in Figure 3.2 through theory and practice. Some small-scale experiments will be performed to relate the theory to practice to create an overview that will help in finding ways of minimising the evaporation effect.

The used methods and tools for this SQ are:
1. Literature analysis on grinding dynamics and heat generation
2. Small scale experiments
3. Internal documents

SQ2 *What are candidate solutions for reducing the evaporation effect in the grinder?*

After the identification of the system dynamics, the main contributors to the production loss are known and enable us to investigate the possible ways (or artefacts) of minimising the evaporation effect denoted as *candidate solutions*. These candidate solutions will be subjected to a quick analysis by grading their expected effects against the most important (weighted) stakeholder requirements. The results will be represented in a solutions design matrix with an overall score per solution, such that a decision can be made on which ones should be investigated in more depth. This whole process will be done in collaboration with the relevant stakeholders.

The used methods and tools for this SQ are:
1. Weighted solutions design matrix
2. Results from the dynamical analysis
3. Initial estimations on the effect of solutions
4. Discussion with stakeholders

SQ3 *What is the best way to reduce the loss due to evaporation?*

Based on the results from the identification of candidate solutions, an in-depth analysis will be performed on the most promising solutions, such that their real impact can be determined in terms of loss reduction, increase in revenue and their accompanying costs. From these candidate solutions, the best solution will be proposed by re-creating the solutions design matrix, with more accurate estimates on their impact on the weighted stakeholder requirements. Based on this solutions design matrix, the best candidate solution will be chosen and implemented. This whole process will again be done in collaboration with the relevant stakeholders.

The used methods and tools for this SQ are:
1. Loss reduction calculation
2. Revenue increase calculation
3. Yearly savings calculation
4. Experiments on GRIN01 (DoE: RSM)
5. Weighted solutions design matrix
6. Discussion with stakeholders

SQ4 *How should the solution be implemented?*

Here the focus will be on *how* the implementation of the solution should be done. This is again done in collaboration with the relevant stakeholder and possible vendors that are involved.

> The used methods and tools for this SQ are:
> 1. Discussion with stakeholders
> 2. Contacting vendors for new machines

SQ5 *What are the new parameter setting to meet all the stakeholder requirements?*

After implementation of the solution in (or on) the grinder systems, the dynamics of the systems might differ from the initial setting. Therefore, to find the new optimal setting for the grinder to meet all the requirements, response surface methodology will be used.

> The used methods and tools for this SQ are:
> 1. Experiments on the new system (DoE: RSM)

SQ6 *What is the eventual loss reduction and yearly savings as a result of the new measure and its settings?*

To conclude the research, the predicted loss reduction is evaluated by taking measurements after the solution has been implemented and optimised in terms of settings. It will be a comparison study of the old data, the original experiments and the new experiments.

> The used methods and tools for this SQ are:
> 1. Monitoring the loss reduction
> 2. Savings calculation based on old data and new results
> 3. Evaluation of the implemented solution
> 4. Verification of predicted loss reduction

Based on these research questions, this research will be structured as follows: Section 5 is dedicated to give a thorough literature analysis as a basis for SQ1-3. In Section 6, the dynamics of the current system are described, resulting in the identification of candidate solutions answering SQ1-2. Next, Section 7 analyses a selection of these candidate solutions, to propose a solution for Tripper Nature, hence answering SQ3. After that, Section 8 describes the evaluation of the implemented solution, to determine the consequent loss reduction and yearly savings, answering SQ4-6. In Section 8.3, the research is concluded followed by a discussion and future extensions.

4.4 Project Planning

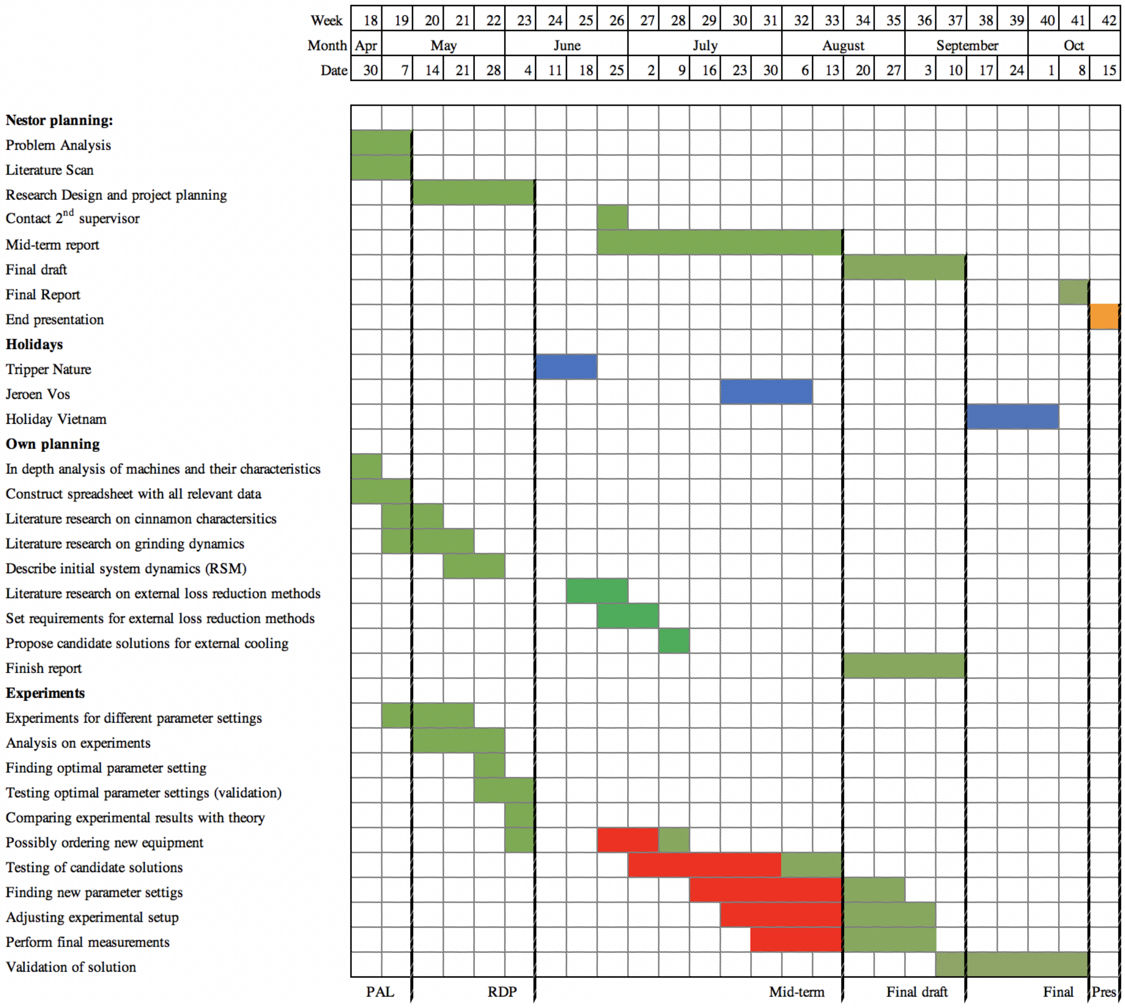

Figure 4.3: Gantt chart of the project planning.

5 Literature Research

By using Hevner's three-cycle view as the backbone of this research, this chapter takes place in the rigor cycle, which according to Hevner (2007), is necessary for the selection of appropriate theories and methods that are relevant for constructing and eventually evaluating the to-be-designed artefact or solution.

As mentioned in Section 3.3, the main cause to the production loss is the evaporation effect due to high temperatures in the grinder. Therefore, we will look into the theoretical characteristics of grinding and find a way to describe its dynamics. Hence, this section will shed some light on grinding characteristics and a way to statistically describe the dynamics through of Response Surface Methodology.

5.1 Grinding Characteristics

Grinding is one of the most common size reduction operations used in the food industry. At the surface, it is a relatively easy production step; reducing material from an initial size, into the desired output size by applying a force on the material such that it breaks into smaller pieces. However, the dynamics behind grinding are extremely complex since many factors have to be taken into account such as the material type, material properties, the initial size, output size, grinder specifications and external factors. Below, a review is given on the theory behind breaking material, together with general laws that describe the total required energy.

5.1.1 Materials under stress

In grinding, three types of forces can be implied on the material to induce stress: 1) compression force, 2) impact force and 3) shear force. Dependent on the grinding equipment used, one of these three forces is paramount while the other two forces will have a lesser impact. As discussed in Section 3.3, the air-swept pulveriser is mainly based on impact force.

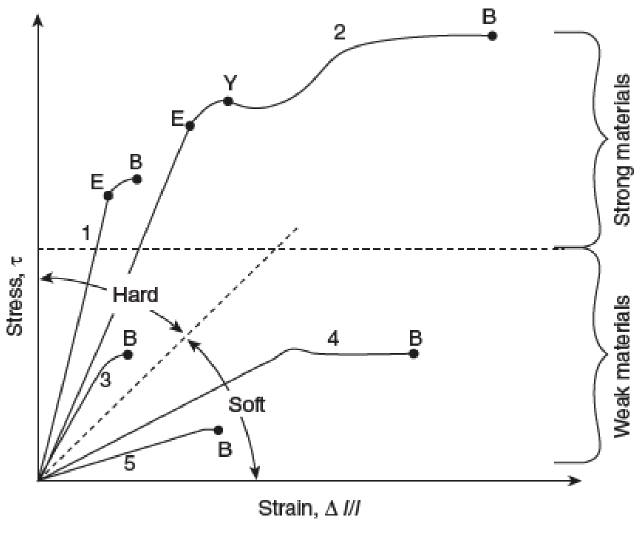

Figure 5.1: Stress-strain for different materials (Rahman and Ahmed, 2012).

Figure 5.1 show the stress-strain curves for different types of materials and will be used to explain the behaviour of materials under stress. By applying force (stress) to the material, the internal strain will increase proportionally (linearly) to the stress, as long as it stays below a material specific elastic stress limit E. Within this region the material will return into its original shape when the force is removed, called the elastic region (O-E). However, if the strain in a local area exceeds the elastic stress limit E, the material will start to permanently deform due to fractures along weak lines in the material, called plastic deformation (region E-B). If even more force is applied, the deformation will exceed a certain critical point after which the material breaks (point B) (Rahman and Ahmed, 2012).

The function for stress in elastic material can be used to approximate the required work for breaking material. It is defined as $\tau = E\Delta$, where E is the Young's modulus (or the slope) and Δ is the strain (or deformation). The material breaks after reaching a certain maximum stress level τ_B which depends on the hardness and friability (tendency to crack) of the material. Mathematically, the amount of work per unit of mass can be approximated by the proportional integral

$$\int_{\tau}^{\Delta} E\Delta \, \mathrm{d}\Delta = \frac{1}{2}E\Delta^2. \tag{5.1}$$

Up until the point of breaking, the energy as a function of deformation $\frac{1}{2}E\Delta^2 \propto \frac{\tau^2}{E}$. It shows that the required work is proportional to the square of the material strength (τ_B), and inversely proportional to the Young's modulus. This means that it is difficult to break material with high resistance to breaking and low resistance to deformation (ductile material), while brittle material needs only a small deformation to break. In general, the total work for ductile materials is often higher compared to brittle materials (Rahman and Ahmed, 2012).

5.1.2 Energy requirements

For calculating the required energy of grinding, three theories (or laws) are used frequently for different situations. They are named after the persons who invented the laws: Kick, Rittinger and Bond. The three laws are all based on a general equation that relates the change in required energy to the change in the size of the material by

$$\frac{\mathrm{d}E}{\mathrm{d}x} = \frac{-K}{x^n}. \tag{5.2}$$

$\mathrm{d}E$ is the required energy for a change $\mathrm{d}x$ in the size of the material. x is the size of the material, n is an exponential factor representing the dimensions of the size (differs per law) and K is the constant that depends on the material and equipment. The total energy is measured per unit mass of the input material (kWh/ton) (Saravacos et al., 2002).

Kick

The Kick law states that the required energy for the size reduction of material is proportional to the ratio between the initial size and the final size of the material in one typical dimension (e.g. the longest radius of a particle). Since only one typical dimension is considered, the exponential term $n = 1$ results in the integrated equation

$$E = K_K \ln\left(\frac{x_1}{x_2}\right), \tag{5.3}$$

where E is the required energy per unit mass, K_K is the Kick's constant, x_1 is the average initial particle size and x_2 is the final particle size. In general, Kick's law is used in to calculate the required energy for course grinding.

Rittinger

Rittinger's law considers the required grinding energy as being proportional to the change in surface area of the ground product e.g. a two-dimensional relationship $n = 2$. The solved differential equation from initial to final particle size then becomes

$$E = K_R\left(\frac{1}{x_2} - \frac{1}{x_1}\right), \tag{5.4}$$

where K_R is the Rittinger's constant and x_1, x_2 are again the mean sizes of the input and output material. This law gives better results for energy calculation of fine grinding, since it will increase the total surface area significantly (Saravacos et al., 2002).

Bond
Bond's law is used for energy calculation for particles from very large initial mean size to very small size by taking $n = 3/2$ such that the integrated equation becomes

$$E = K_B \left(\sqrt{\frac{1}{x_{(80)2}}} - \sqrt{\frac{1}{x_{(80)1}}} \right). \tag{5.5}$$

Note however that Bond's definition for particle size different. The 80 in x_{80} stand for the requirement that 80 % of the input and output material should pass through sieves of a specific size.

In practice, Rittinger's law is most frequently used in the food industry while the Bond's and Kick's law were originally developed in the studies of hard materials in the mining industry. It is important to note that the K constants of the laws are unique for every situation since they incorporate all the material properties and the grinder specifications. The only way to determine such a constant is by ways of experimentation where the total input energy, input size and output size should be known.

5.1.3 Dissipated heat energy during breaking

In general, the process of grinding is extremely inefficient where only a small amount of the total input energy is used for the actual breaking of the material. The majority of the energy is used for the elastic deformation (before breaking), the creation of cracks and dissipation of energy as a result of breaking (Saravacos et al., 2002). This dissipation of energy is related to the total required work for breaking materials in terms of the total energy density in $\mathrm{Jm^{-3}}$

$$U = U_c + U_e \tag{5.6}$$

that has to be applied by an external force. The total energy density U is a function of the releasable strain energy U_e stored in the material volume and the dissipation energy density U_c during plastic deformation (Fan et al., 2016). The energy accumulation, dissipation and release of energy is graphically represented in Figure 5.2.

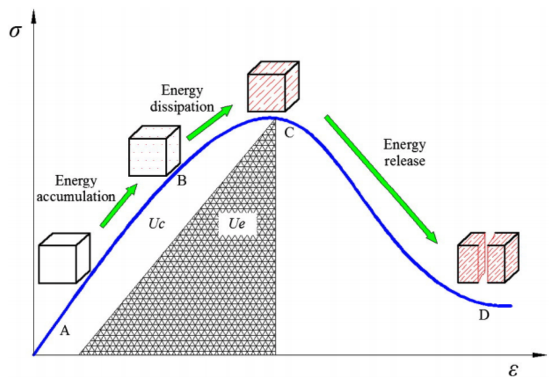

Figure 5.2: The energy density of a mass volume (Fan et al., 2016).

Since the dissipation of energy occurs during the plastic deformation (B-C), the amount depends on the resistance to breaking of the material. Cassia cinnamon is considered as a brittle material with an average resistance to breaking, meaning that the region of plastic deformation will be relatively small (Ravindran et al., 2003). This small region of plastic deformation results in a low contribution of dissipated energy to the total heat production. However, based on the unit of dissipated energy density $\mathrm{Jm^{-3}}$, it should be noted that during the production of large volumes, the contribution of dissipated energy to the total heat production in the system increases.

5.2 Response Surface Methodology

To study the response of a system to different input variables, one way is to construct its dynamical equation incorporating all different variables that are involved in the process. By analysing this dynamical equation, the responses of a system to certain variables can be identified using simulations, such that optimal setting can be found. However, this process of creating the dynamical equation is in many cases too difficult to perform because of complex interactions between the variables and their effect on the output. Fortunately, there is a collection of mathematical and statistical techniques available originating from Design of Experiments (DoE) that is able to describe the input-output response of a system without giving a full description of the dynamical system: Response Surface Methodology (RSM) (Davim and Aveiro, 2016).

5.2.1 Preliminaries

RSM considers the system as a black box with different inputs (called factors) and outputs (the response). It tries to approximate the functional relationships between these variables through regression analysis for the range of expected variation in the inputs (Morshedi and Akbarian, 2014). Mathematically, this means that the output response y is related to a k number of input variables $x_1, x_2, ..., x_k$ approximated by the low-degree polynomial

$$y = f(\mathbf{x})\boldsymbol{\beta} + \boldsymbol{\epsilon} \tag{5.7}$$

where $f(\mathbf{x})$ is a vector function of p elements that consists of powers and cross-products of powers of $\mathbf{x} = [x_1, x_2, ..., x_k]^{\mathrm{T}}$, up to a certain degree $d \geq 1$. The vector $\boldsymbol{\beta}$ contains the coefficients for all p elements and $\boldsymbol{\epsilon}$ represents the noise or error observed in the response. The function that describes the relationship between the input and the output can be a simple linear or factorial model, but can also be a more complex quadratic function (Khuri and Mukhopadhyay, 2010). The first order model ($d = 1$) is given by

$$y = \beta_0 + \sum_{i=1}^{k} \beta_i x_i + \epsilon \tag{5.8}$$

and the second-order model ($d = 2$) is given by

$$y = \beta_0 + \sum_{i=1}^{k} \beta_i x_i + \sum_{i<j}\sum \beta_{ij} x_i xj + \sum_{i=1}^{k} \beta_{ii} x_i^2 + \epsilon. \tag{5.9}$$

It shows that the first order model represents a simple linear relationship between the inputs and the response, while the second order also shows an interaction between input variables and quadratic terms. RSM aims to fit these linear or non-linear functions to the response surface model for the number of inputs, such that a description of the system dynamics can be given up to a certain statistical significance.

The construction of the model starts with a n number of experiments where the response y of the system is measured for specific settings of input variables. The response surface design is based on the totality of these input variables, represented by the *design matrix*,

$$D = \begin{bmatrix} x_{11} & x_{12} & \dots & x_{1k} \\ x_{21} & x_{22} & \dots & x_{2k} \\ \vdots & \vdots & \ddots & \vdots \\ x_{n1} & x_{n2} & \dots & x_{nk} \end{bmatrix} \tag{5.10}$$

with an order of $n \times k$. This means that for every k input variable (factor), a n number of values (or levels) can be picked for experimentation, referred to as a n^k factorial design. In the design matrix, every row represents a specific combination of input variables, called a *design point*.

It is important to note that in RSM analysis, all natural input variables are converted into coded variables such that the estimated intercept will be in the centre of the design space, making the results easier to interpret. The coded variables are determined by

$$x_i = \frac{x_i - [\max(x_i) + \min(x_i)]/2}{[\max(x_i) - \min(x_i)]/2} \tag{5.11}$$

to take the values, -1, 1 and 0 for the low, high and centre level of each variable (Morshedi and Akbarian, 2014). After the analysis, the natural values can be recalculated to correspond to real input values.

Based on the coded design points and their corresponding response, the RSM will try to describe the dynamics of the systems through first/second order regression fit (Khuri and Mukhopadhyay, 2010). The statistical significance of the response surface model is checked by use of Analysis of Variance (ANOVA) between the real and modelled response and the regression models are analysed based on the Fisher F-test with a 95% confidence interval (Morshedi and Akbarian, 2014).

An (uncoded) example of a well fitted response surface is shown in Figure 5.3, where the strength of cement is given as a function of calcination temperature and residence time.

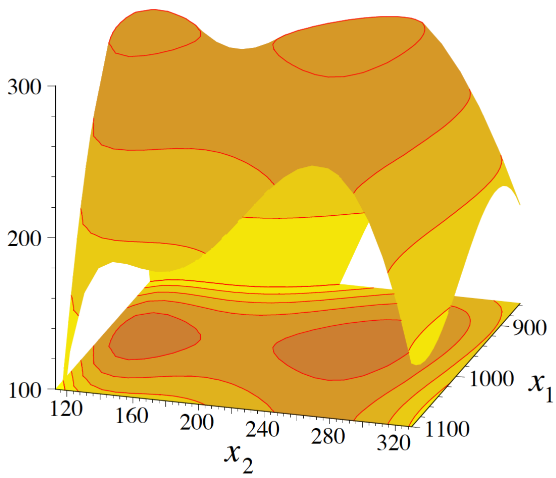

Figure 5.3: 3D response surface of the strength of cement (y) as a function of calcination temperature (x_1) and the residence time (x_2) (Alvarez, 2000).

5.2.2 Design of Experiment: The Central Composite Design

The methodology behind RSM enables researchers to perform experiments in a very structured manner, such that the minimal number of tests can be performed, whilst ensuring a high statistical significance for the regression fit of the response surface. In most cases (and also for this research), a second-order design is needed to describe the dynamics of the system, because a linear model does not fit the dynamics. The most popular second-order design is the so-called Central Composite Design, which is a combination of a first-order and a second-order design.

The graphical representation of the CCD design matrix D is shown in Figure 5.4. The four blue corner-points (design points) of the square augment the first-order design, called a 2^k factorial design. In this case there are $k = 2$ factors (x_1 and x_2) with only $n = 2$ levels, coded as -1, 1 (minimum and maximum). This first-order design is used to get initial information about the behaviour of the response as a result of extreme values and shows the significant impact of the factor (or not). In addition to the first-order design points, $2k$ axial points (red) are added to the design of experiment on the grey circle with a radius of $\sqrt{2}$. Furthermore n_0 centre-point (black) replications are added. For these centre-points, it is common to use multiple measurements to reduce possible variance and increase the fit of the model in the F-test. The use of axial- and centre-points in addition to the first-order corner points, leads to a second-order design with more information about the behaviour of the system and enables a researcher to determine optimum conditions (Khuri and Mukhopadhyay, 2010).

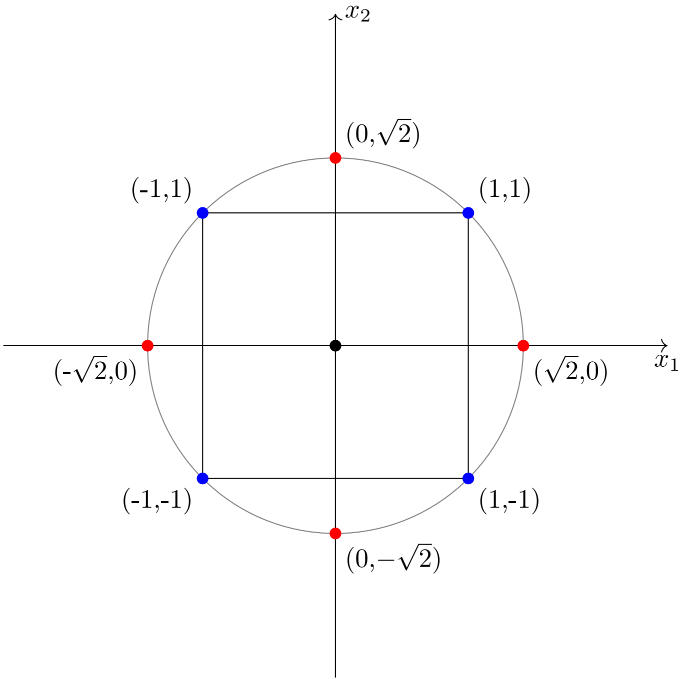

$$D = \begin{bmatrix} -1 & -1 \\ 1 & -1 \\ -1 & 1 \\ 1 & 1 \\ -\sqrt{2} & 0 \\ \sqrt{2} & 0 \\ 0 & -\sqrt{2} \\ 0 & \sqrt{2} \\ 0 & 0 \\ 0 & 0 \\ 0 & 0 \\ 0 & 0 \\ 0 & 0 \end{bmatrix}$$

Figure 5.4: Graphical representation of the CCD design matrix D.

Based on the design matrix D, all thirteen experiment should be conducted with the natural input variables corresponding to the coded ones and registering the response of the system. After the response is logged, several software packages are available for the creation of the response surface, the ANOVA analysis, the F-test and to find the optimal conditions. In this research, the Design Expert software package (version 7.0.0 [Dx7] Stat-Ease, Inc., Minneapolis, MN, USA) is used for the total analysis of the experiments.

6 System Dynamics: Establishing the Total Power Flow

For this chapter, we shift our focus more towards the design cycle as to eventually generate design alternatives by using our theoretical knowledge base from the rigor cycle, whilst combining it with requirements and field observations from the relevance cycle (Hevner, 2007).

To structure this chapter, we extend the initial causal model in Figure 3.2 into Figure 6.1 to get a better understanding of the grinding dynamics, such that we can propose candidate solutions in accordance with the stakeholder requirements. The extended causal model is based on literature, field observations, experiments and contact with the supplier of the grinder.

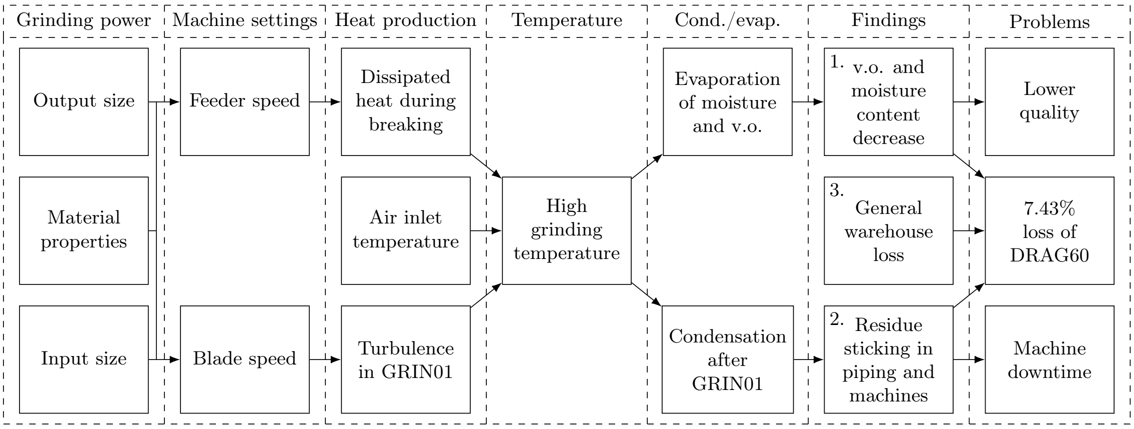

Figure 6.1: Causal model to identify all influencing factors to the high temperatures in GRIN01.

In Section 3.2, we were able to conclude that the production loss of DRAG60 is mainly the result of the evaporation effect of moisture and volatile oil due to high grinding temperatures. The newly found causes to these high temperatures are categorised in *heat production*, *machine settings* and *grinding power* which also correspond to the sections below for further explanation. The goal of the following sections is to quantify the impact of all the causes as much as possible and determine how the total power flows through the grinder, such that multiple candidate solutions can be proposed. The impact of these candidate solutions will be initially graded against the stakeholder requirements in a weighted solutions design matrix, such that a tangible overview is created to assists in identifying the most suitable candidate solution that should be subjected to an in-depth analysis.

6.1 Heat production in GRIN01

Since the grinding temperatures are the direct effect of heat production, we should identify these heat sources and quantify their impacts. The heat produced in the grinder can be attributed to three main factors: turbulence in the grinder, the dissipated heat during the breaking of cinnamon and the air inlet temperature. Therefore, this section will first discuss how the total heat production in the grinder can be approximated in general, to then further determine the impact of each of the three factors on the total heat production.

6.1.1 General expression for heat production and the total production

Since the installed grinder at Tripper Nature uses air to transport the ground cinnamon from the grinder to the product collector, there is an airflow going into and out of the grinder. The air temperatures are constantly monitored by a (calibrated) thermometer at the air inlet and a thermometer placed inside the piping, directly after the grinding area. The difference between the inlet temperature and the outlet temperature can be used to determine the heat production in GRIN01.

The heat balance and assumptions
To do so, the general balance equation from the field of physical transport phenomena described by den Akker and Mudde (2014)

$$\frac{\mathrm{d}VX}{\mathrm{d}t} = \phi_v X|_{\mathrm{in}} - \phi_v X|_{\mathrm{out}} + r_X, \tag{6.1}$$

is transformed into the general heat balance by using $X = \rho C_p T$ and $r_X = \phi_q + \phi_w$ to get

$$\frac{\mathrm{d}V\rho C_p T}{\mathrm{d}t} = \phi_v \rho C_p T|_{\mathrm{in}} - \phi_v \rho C_p T|_{\mathrm{out}} + \phi_q + \phi_w \tag{6.2}$$

where:

V = The control volume [m^3]
ρ = The density of the considered fluid/gas [$\mathrm{kg} \cdot \mathrm{m}^{-3}$]
C_p = The heat capacity [$\mathrm{J} \cdot \mathrm{kg}^{-1} \cdot {}^\circ\mathrm{C}^{-1}$]
T = The temperature [$^\circ$C]
ϕ_v = The flowrate [$\mathrm{m}^3 \cdot \mathrm{s}^{-1}$]
ϕ_q = The heat transfer with environment [$\mathrm{J} \cdot \mathrm{s}^{-1}$]
ϕ_w = The production term [$\mathrm{J} \cdot \mathrm{s}^{-1}$].

For the calculation, Figure 6.2 represents the grinder in Appendix C, in a simplified way as a container with an in- and outflow of air, equipped with a heating element ϕ_w and heat loss to the environment ϕ_q. By calculating the generated heat of this fictional element, the total heat production of the grinding process can be estimated.

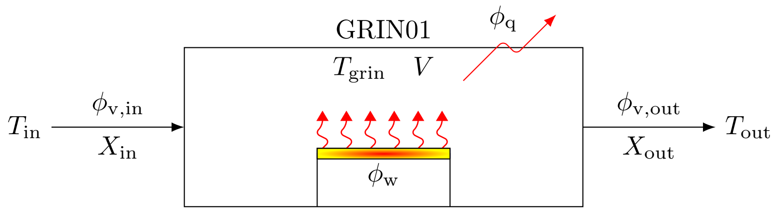

Figure 6.2: Schematic representation of heat production in GRIN01.

For the calculation, the following two assumptions are made:

1. The grinding process is perfectly stirred and in steady-state, i.e. $T_{\mathrm{grin}} = T_{\mathrm{avg}} = T_{\mathrm{out}}$, $\frac{\mathrm{d}VX}{\mathrm{d}t} = 0$, $X_{\mathrm{in}} = X_{\mathrm{out}}$ and $\phi_{\mathrm{v,in}} = \phi_{\mathrm{v,out}}$.
2. The heat loss to the environment is assumed to be modelled by an air-iron-air configuration: the hot air in the grinding chamber loses heat through the iron casing to the ambient air. The total heat transfer is then described by $\phi_q = -UA(T_{\mathrm{grin}} - T_{\mathrm{amb}})$, where U is the heat transfer coefficient, A is the casing surface area and T_{grin}, T_{amb} represent the temperature inside and outside the grinder.

Based on these assumptions, the expression for the heat production ϕ_w in GRIN01 can be obtained by rewriting Equation 6.2 into

$$0 = \phi_v \rho C_p (T_{\mathrm{in}} - T_{\mathrm{out}}) - UA(T_{\mathrm{grin}} - T_{\mathrm{amb}}) + \phi_w, \tag{6.3}$$

$$\phi_w = -(\phi_v \rho C_p + UA)(T_{\mathrm{in}} - T_{\mathrm{out}}) \tag{6.4}$$

$$\phi_w = (\phi_v \rho C_p + UA)\Delta T. \tag{6.5}$$

Note that $\Delta T = T_{\mathrm{out}} - T_{\mathrm{in}}$. With this equation, it becomes possible to determine the heat production in the grinder.

The total heat production

To estimate the total heat production of the system, a two-hour grinding experiment is conducted with the default settings for DRAG60: blade speed 1650 RPM, feeder speed 40 RPM and 1800 kg WIP input material. By monitoring the inlet and outlet temperature during production, it becomes possible to identify the steady-state temperature difference during production $\Delta T_{\text{ss, prod}}$. The development of the temperature difference between the inlet and outlet temperature is plotted in Figure 6.3. It shows that the temperature stabilises at $\Delta T_{\text{ss, prod}} = 25.7$°C after about 45 minutes.

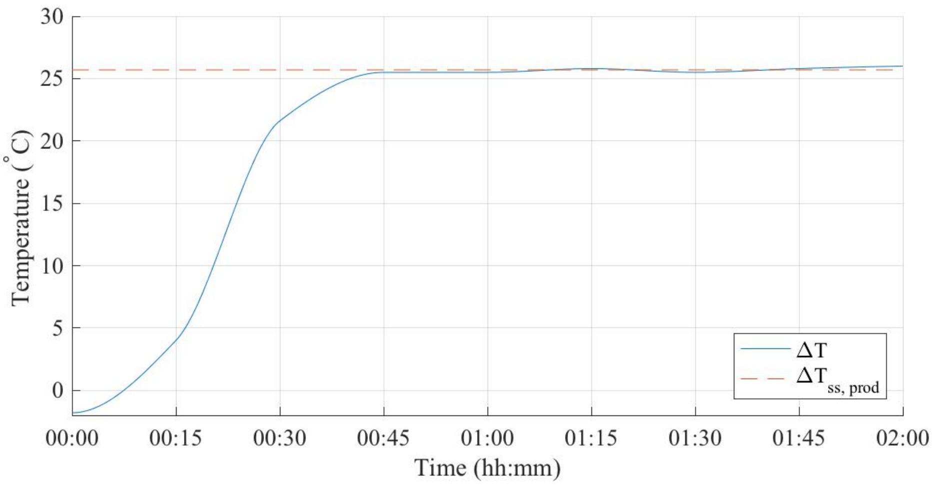

Figure 6.3: Temperature stabilisation (steady-state) during production of DRAG60.

With this stabilised temperature difference, the assumption of steady-state becomes true and Equation 6.3 can be used to calculate the total heat production using the following variables from field observation and literature:

$\rho_{\text{air}} = 1.1455\ \text{kg} \cdot \text{m}^{-1}$ (at 33 °C)
$C_{p,\text{air}} = 1.008\ \text{kJ} \cdot \text{kg}^{-1} \cdot {}^{\circ}\text{C}^{-1}$
$\Delta T = 25.7\ {}^{\circ}\text{C}$
$\phi_v = 1.005\ \text{m}^3 \cdot \text{s}^{-1}$
$U = 7.9\ \text{W} \cdot \text{m}^{-2}{}^{\circ}\text{C}^{-1}$ (den Akker and Mudde, 2014)
$A = 2.316\ \text{m}^3$

With these variables, the estimated heat production in GRIN01 for producing DRAG60 becomes at least $\phi_w \geq 30.4$ kW, of which 405 W is heat loss to the environment (about 1.3%). Note however, that the calculated amount of produced heat does not correspond to the actual heat production in the grinder. This is because the calculated amount is based on the temperature difference of the inlet and outlet temperature of air only. Since the generated heat in the grinder is absorbed by the air *and* the cinnamon, we cannot state that the found produced heat energy is the actual amount. However, by knowing the (estimated) total heat production it becomes possible to determine the proportional impact of the individual causes of turbulence, dissipation and inlet temperature.

6.1.2 Turbulence in GRIN01

The heat production of turbulence is expected to have the biggest impact since initial observations during the experiments showed that the temperature in the grinder increases drastically even in the absence of input material. No direct explanation was found in literature, after which Reynolds Engineering & Equipment was consulted to give an explanation on this matter. They referred to the operation manual, present at Tripper Nature, and pointed out that this initial heat production in the grinder is because of the created turbulence between the rotating beater plates and the lining (as introduced in Section 3.3.2). The acceleration and collision of air molecules in the grinder increases their internal energy and thus generates heat in the grinder (Reynolds Engineering & Equipment, 2001).

Based on this knowledge, it is of interest to quantify the contribution of heat production due to turbulence to the total heat production of 30.4 kW. To do so, a new two-hour grinding experiment is conducted, but now without any input (feeder speed 0 RPM). The temperature development is plotted in Figure 6.4 and shows a temperature development similar to the producing grinder, but it stabilises at $\Delta T_{\text{ss, turb}} = 24$°C after 30 minutes.

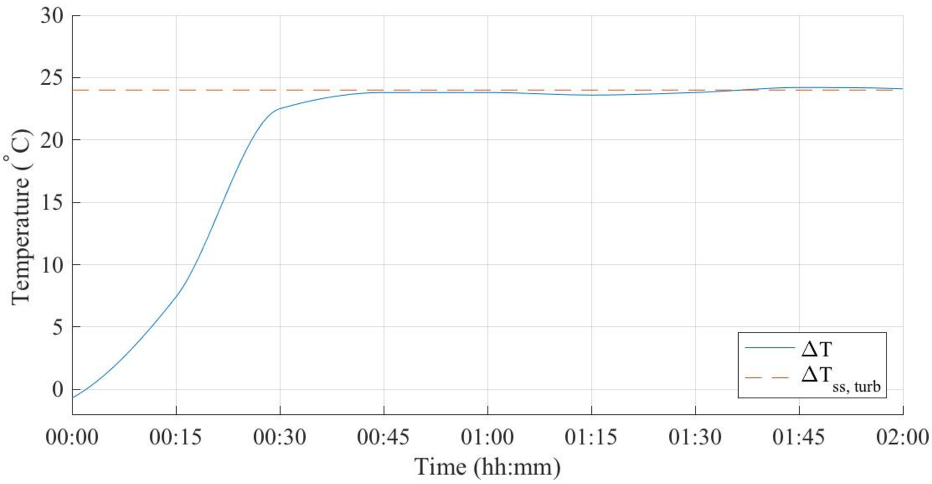

Figure 6.4: Temperature stabilisation (steady-state) without cinnamon input.

By inserting the newly found steady-state temperature in Equation 6.3, the total heat production due to turbulence is estimated to be $\phi_{\text{w, turb}} = 28.4$ kW. Based on the estimation of the total heat production in the previous section, this means that the proportional contribution of the turbulence is $C_{\text{turb}} \leq 93.4\%$.

6.1.3 Dissipated heat during breaking

As introduced in Section 5, the actual breaking of material creates dissipated heat. Although this effect is minimal for small volumes, its impact on the total heat production during grinding starts to increase for bigger production volumes. Based on the calculated contribution of turbulence on the total heat production for DRAG60, it can be concluded that the contribution of dissipated heat is $C_{diss} \geq 100\% - 93.4\% \geq 6.6\%$, resulting in $\phi_{w,diss} \geq 2.0$ kW. To support this calculation, the experiment (with no input) in the previous section was extended by turning on the feeder at 40 RPM after the initial two hours of running the empty grinder. The temperature development is plotted in Figure 6.5 and indeed shows a sudden increase from $\Delta T_{\text{ss, turb}} = 24$°C to about $\Delta T_{\text{ss, prod}} = 25.7$°C. By inserting this temperature increase of 1.7°C into Equation 6.3 we indeed find the 2.0 kW heat production due to the dissipation of energy. Keep in mind that this is again only the heat absorbed by the air, so the actual dissipation is expected to be higher.

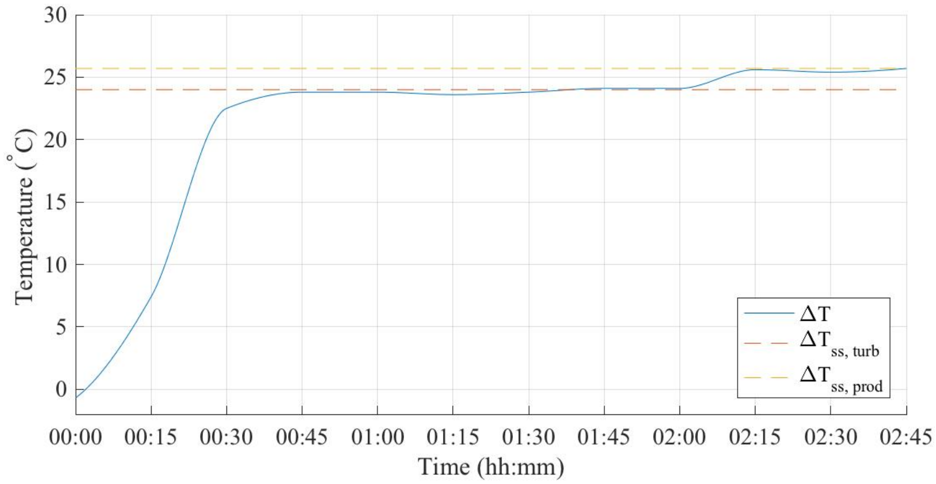

Figure 6.5: Temperature stabilisation (steady-state) before and after input of cinnamon.

6.1.4 Air inlet temperature

Based on Equation 6.3, the air inlet temperature also shows to be of great influence on the grinding temperature. Since the factory is based in Jakarta, this leads to a disadvantage due to the high average ambient temperature of 32°C. Furthermore, since the grinder is placed in a closed room, the heat production in the grinder and its heat transfer with the environment leads to an increase in room temperature during production. The impact of this effect is measured by two equally calibrated thermometers in the grinding room and the factory itself during eleven batch productions. The results were that on average, the ambient temperature in the factory raised by 0.4 °C/h while the temperature in the grinding room raised by 1.19 °C/h. Since the grinder sucks in the air from the room, this temperature increase in the room also increases the effective grinding temperature inside the grinder during the day.

Figure 6.6 shows the relation between the inlet temperature (T_{in}) and the outlet temperature ($T_{\mathrm{out}} = T_{\mathrm{grin}}$) based on Equation 6.3.

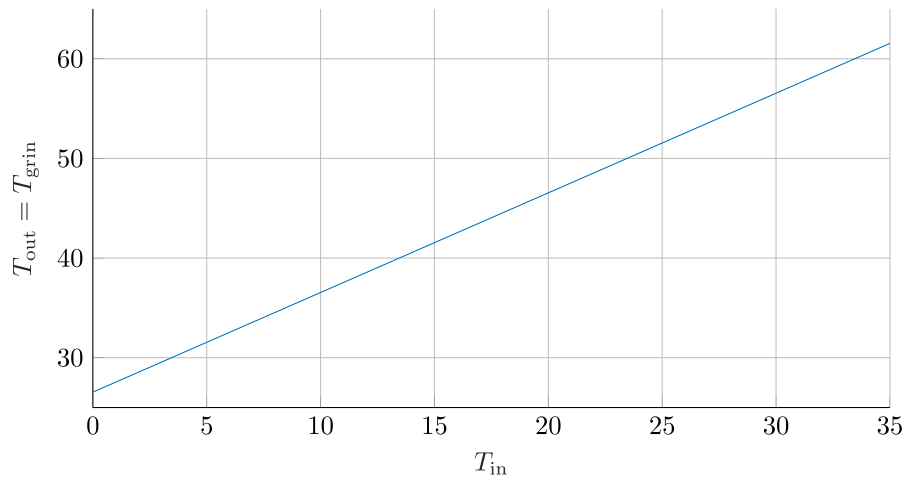

Figure 6.6: Output temperature estimation as a function of varying input temperature.

6.2 Machine Settings

Figure 6.1 indicates that the machine settings are directly related to the production of heat in the grinder. The two sections below determine the causal relationship between settings and heat production.

6.2.1 Blade speed

Since we already established that the contribution of turbulence to the total heat production is around 93%, it is interesting to see how the heat production develops as a result of different rotating speeds. Therefore, we conducted an empty experiment that registered the temperature difference ΔT between the air inlet and outlet for blade speeds ranging from 150 RPM - 1650 RPM in steps of 250 RPM. The speed is increased once the temperature was registered at a steady-state temperature difference ΔT_{ss}. Furthermore, the flow rate of the air inflow was measured for every setting since it slightly differs and impacts Equation 6.3. The development of heat production as a function of increasing blade speeds is shown in Figure 6.7 together with a nonlinear trendline with a coefficient of determination of $R^2 = 0.995$.

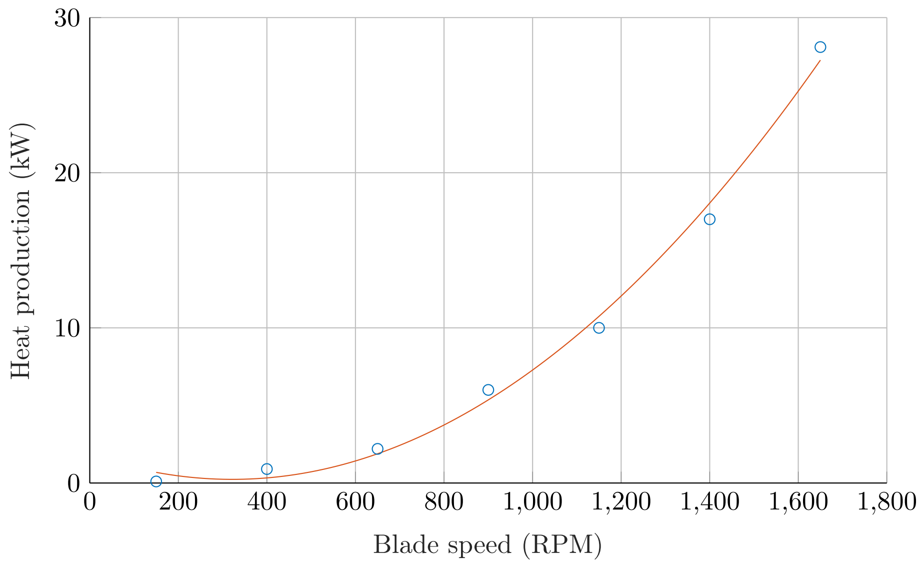

Figure 6.7: The nonlinear relation between the rotating speed of the blades and the heat production.

6.2.2 Feeder speed

As introduced in Section 5, the volumetric inflow of the material into the grinder contributes to the total amount of dissipated heat due to breaking. Therefore, the feeder speed is expected to also impact the total heat production since it dictates the volumetric inflow of cinnamon. To see the impact of the feeder speed on the loss, we conducted a total of four experiments where the blade speed is set at 1650 RPM and the feeder speed is increased from 25 RPM to 40 RPM in steps of 5 RPM. The scatter plot of the registered loss is shown in Figure 6.8 together with a second-order polynomial with $R^2 = 0.93$. It shows an interesting non-linear behaviour between the loss and the feeder speeds, where the loss decreases for lower feeder speeds, except for the lowest feeder speed. A possible explanation for this behaviour can be found in the fact that the inflow of cinnamon is also expected to influence the heat absorption per cinnamon particle. In a scenario where the inflow of cinnamon is very low, fewer particles are present in the grinding area to absorb the present heat created by the turbulence. Therefore, it is expected that the heat absorption per particle will be higher, hence evaporating more moisture and volatile oil. Therefore, the increase in loss for low feeder speeds might be due to a certain trade-off between heat absorption per cinnamon particle and its own heat dissipation, this is however not completely certain.

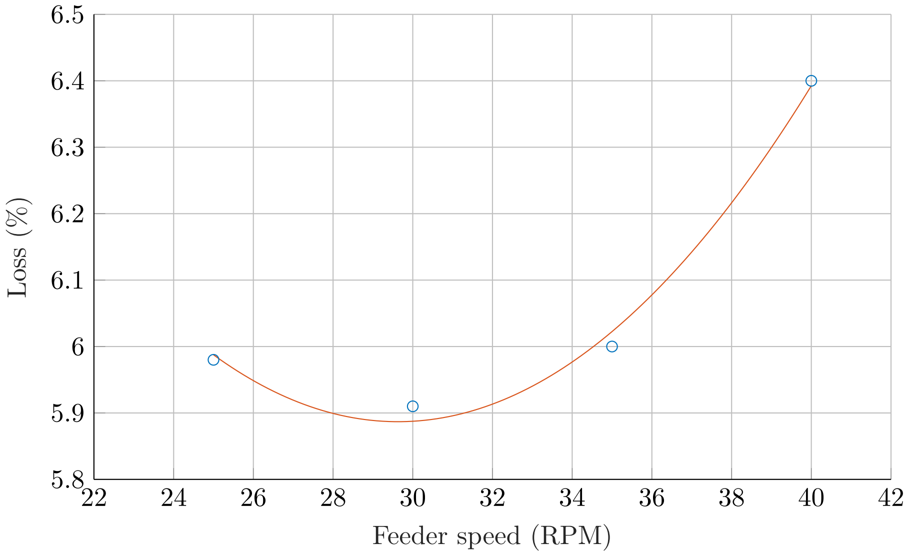

Figure 6.8: The loss as a function of different feeder speeds, blade speed is constant.

6.3 Required Grinding Power

The last causal relationship is categorised under the header of *required grinding power*. This is because a combination of the three factors - input size, output size and material properties - determine the required grinding power leading to specific machine settings.

> Note that we are now talking about grinding *power*, in contrast to the introduced grinding *energy* in Section 5, for following two reasons. The first reason is that since we are interested in how the energy flows through the grinder in a steady state, it is more relevant to describe the flow in terms of power (J/s). This way, we can estimate how the total power input is transformed into grinding power, heat production and other forms. The second reason is that the grinder at Tripper Nature is equipped with a voltmeter and ammeter, which enables us to also quantify the grinding power ($P = U \cdot I$), such that we can determine the Rittinger's constant K_R for further calculations.

Now, to express the Rittinger's law from Equation 5.4 in terms of power, we use the fact that the energy per unit mass E (kWh/ton) can be rewritten as a function of power P (J/s) divided by the feed rate $\dot{m}$ (ton/h), such that the Rittinger's law for power becomes

$$P = \dot{m} K_R \left(\frac{1}{x_2} - \frac{1}{x_1} \right). \tag{6.6}$$

The best way to approximate the Rittinger constant K_R is to measure the specific grinding power P_{grin} for different input sizes x_1, output sizes x_2 and feed rates $\dot{m}$, to get the average constant.

In our case, the motor of the grinder works at a constant voltage of $U = 400$ V and is equipped with an internal control mechanism that adjusts the current I to guarantee a preset blade speed. This control mechanism enables us to determine the specific grinding power by measuring the current before and after the input of cinnamon is turned on. When the input of cinnamon to the grinder is turned on, the breaking of the material will slow down the blade speed, causing the motor to increase its current I to maintain the preset speed. By subtracting the current for an empty grinder (I_{empty}) from the current for a grinder in production (I_{prod}), we are left with the current increase that is induced by the motor to keep the RPM at the preset value, while breaking the cinnamon. In other words, the required current for grinding the material becomes $I_{\text{grin}} = I_{\text{prod}} - I_{\text{empty}}$ and can be used to determine the required specific grinding power by $P_{\text{grin}} = U \cdot I_{\text{grin}}$.

Based on this method, the Rittinger's constant is determined by making measurements on I_{empty} and I_{prod} for three input-output combinations: DRAG02→DRAG60, DRAG02→DRAG50 and DRAG60*→DRAG60, where DRAG60* is a byproduct of GRIN02 production. The results are given in Table 6 together with the predicted value for the P_{Ritt} using $K_R = 1.61$. In Figure 6.9 the predicted required grinding power is plotted for varying input sizes (blue line) to produce DRAG60 and for varying output sizes (red line) with DRAG02 as the input. Although it shows a slight deviation between the theoretical and real required power, it is a useful tool to show the impact of different input and output sizes on the required grinding power.

Table 6: Results for the three input-output combinations to determine K_R.

Input	Output	x_1 (mm)	x_2 (mm)	$\dot{m}$ (ton/h)	P_{grin} (kW)	K_R	P_{Ritt} (kW)
DRAG02	DRAG60	20	0.075	0.9	20.8	1.74	19.3
DRAG02	DRAG50	20	0.135	0.8	9.2	1.56	9.5
DRAG60*	DRAG60	0.23	0.075	0.9	12.4	1.53	13.0
					Mean	1.61	

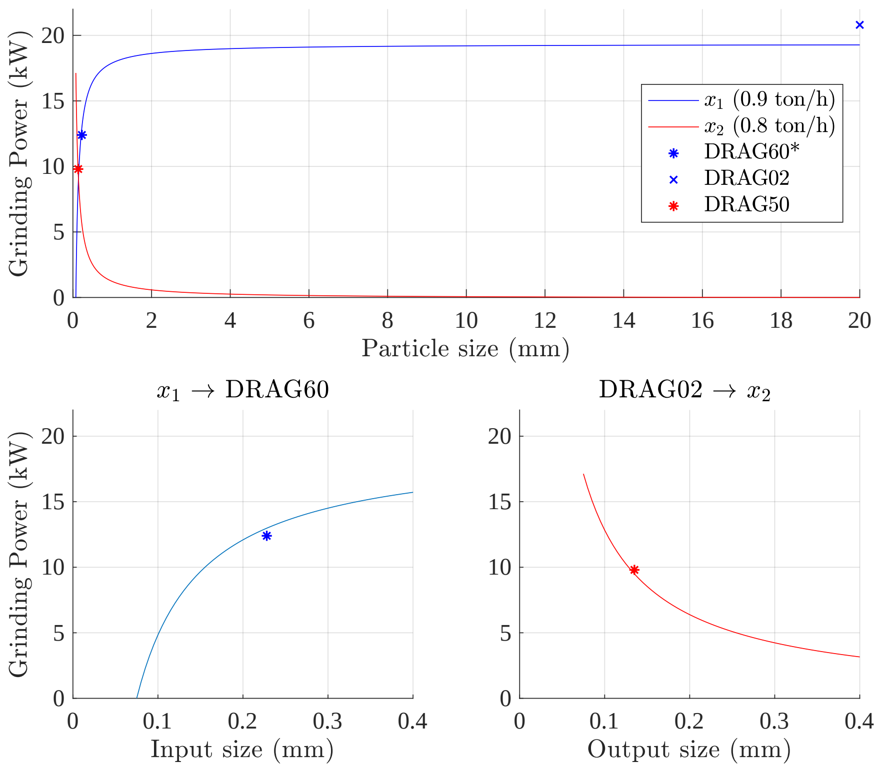

Figure 6.9: Specific grinding power for varying input size x_1 (blue) and output size x_2 (red).

6.4 Total Power Flow

Since the grinder system is an open system (no energy is stored in the system for later use) the input power flows out of the system in different forms, where we know that the total input must equal the sum of outputs under the assumption that the process is in a steady-state. Using this knowledge and the ability to measure the total input power of the motor to run the grinder, we can to some extent validate our previous calculations on the heat production and create a Sankey diagram that shows the flow and transformation of power during the production of DRAG60.

6.4.1 Power flow during DRAG60 production

The Sankey diagram shows the flow of power and its quantification based on the calculated power quantities in the sections above and using the fact that the input must equal the output. The Sankey diagram in Figure 6.10 will be explained below per 'power category', which are subdivided into smaller categories represented by the numbers 1-5. Keep in mind that all the found values are estimations so, in reality, the values might differ, especially for the dissipated heat during breaking.

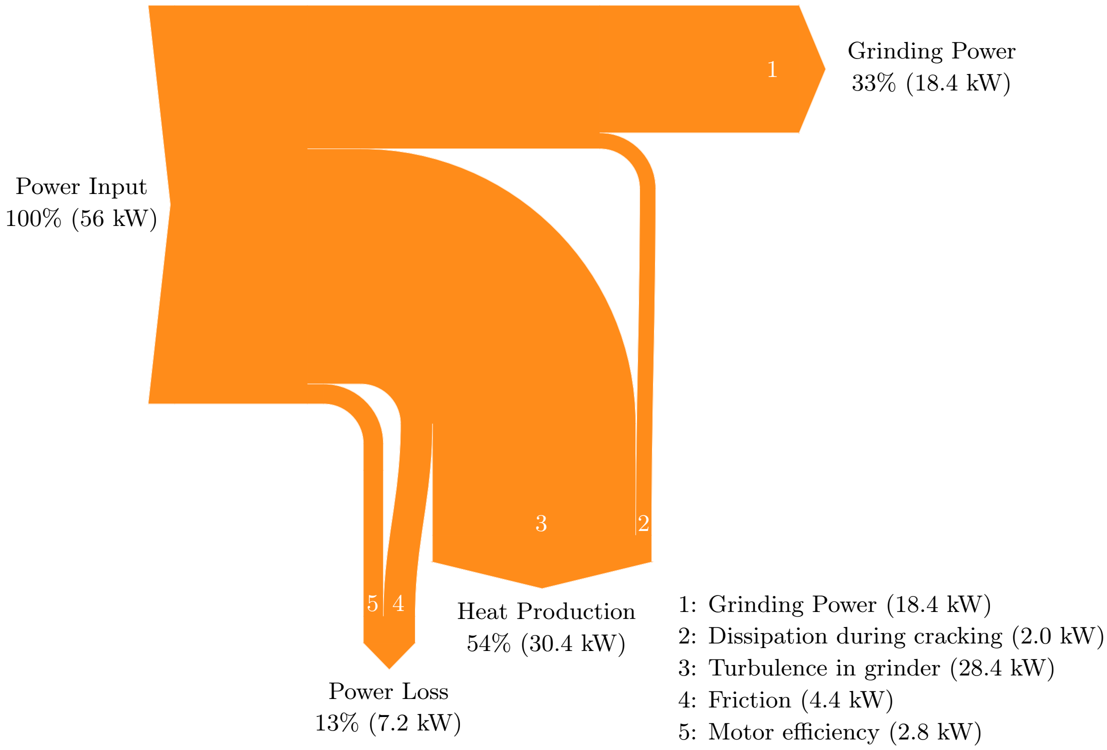

Figure 6.10: Sankey diagram to show the power flow during production of DRAG60.

Power Input
The total power input that is determined by measuring the current on the ammeter during production $I_{\text{prod}} = 140$ A. The current in combination with the constant voltage of $U = 400$ V results in a total input power from the motor of $P_{\text{prod}} = 400 \cdot 140 = 56$ kW.

Grinding Power
The grinding power was calculated to be 20.8 kW, which also included the dissipation of heat at $\phi_{w,diss} \geq 2.0$ kW. Therefore, the actual power that is required for purely breaking of the material (1) comes down to 18.4 kW while the 2.0 kW of dissipated heat flows down to the heat production in the diagram. The amount of power for the actual breaking of the cinnamon accounts for only 33% of the total power input which shows just how inefficient the grinding process is.

Heat Production
In Section 6.1.1, the total heat production was calculated to be $\phi_w = 30.4$ kW as a result of (2) the dissipation of heat during the breaking of the cinnamon at 2.0 kW and (3) the turbulence induced by the beater plates at 28.4 kW. The Sankey diagram shows that the dissipation of energy from the Grinding Power flows down to the Heat Production to add up to the total heat production of 30.4 kW.

Power Loss
This category represents the total loss of power in the system at 7.2 kW which is the sum of the loss due to the 95% efficiency of the motor at 2.8 kW (5) and the loss due to friction in the transmission (4) (Reynolds Engineering & Equipment, 2001). This last amount of loss is calculated to be 4.4 kW by subtracting all the above-calculated powers from the total power input.

6.5 The Solutions Design Matrix

Based on the theoretical analysis of the dynamics of the grinder, several candidate solutions arise that can reduce the total production loss. To initially identify these solutions and to check their feasibility, we created the solutions design matrix in Table 7. It shows an overview of five possible solutions which will be given a score for four weighted KPI's from the stakeholder analysis. The weights and scores are based on discussions with the relevant stakeholders and initial estimations. The eventual score for each candidate solution makes it more tangible, such that a decision can be made on whether we will analyse the candidate solution further on.

Table 7: The weighted solutions design matrix where every candidate solution gets a score between 1-5.

	L	C	P	I	
Weight	0.4	0.3	0.2	0.1	Score
Optimal machine settings	2	5	4	5	3.6
Pre-grinding	2	4	2	5	2.8
Inlet cooling	4	3	5	4	3.9
Cryogenic process cooling	5	1	5	2	3.4
Material cooling	3	2	5	2	3.0

L	Loss reduction
C	Cost minimisation
P	Production rate
I	Implementation

Furthermore, the first two solutions are referred to as *primary* solutions, meaning that they will reduce the loss by directly tackling the root cause; heat production. The other three solutions will be referred to as *secondary* solutions, since they do not take away the root cause of the problem, but rather provide a secondary fix in terms of cooling.

Weight of KPI's
After discussion with the relevant stakeholder, the most essential KPI for each candidate solution would be its achieved loss reduction. This is why the weight factor for *Loss reduction* is set to 0.4. Another important aspect to consider is whether the candidate solution is financially feasible. This *Cost minimisation* KPI is of course closely related to the expected loss reduction since its impact should be significant with respect to the accompanying costs. For this reason, the weight factor for costs is set at 0.3. A third KPI that should be taken into account is whether the *Production rate* is affected by the proposed solution. Although there is room for a higher utilisation rate of GRIN01, it is something to take into consideration since a lower production rate will result in intensified planning. Therefore its weight is set at 0.2. The last KPI is of less importance, but should also be considered: *Implementation.* If the implementation of a candidate solution requires a production stop of the production line or a significant change to the factory, the production engineer mentioned that this would be undesirable.

A stakeholder requirement that is not included, is the quality specification for granulation and minimal moisture and volatile oil content. This requirement can not be expressed in a score since the specifications are met or not met. Therefore, while conducting all experiments, the quality will be checked and reported on if the standard is not met.

Machine settings, score: 3.6
The first and most straightforward candidate solution would be to check whether the current parameter settings of the grinder are actually optimal for grinding DRAG60. The cinnamon business manager mentioned that these settings have been determined two years ago, without using a systematical testing methodology. This means that a loss reduction could be achieved by optimising the machine settings for the lowest loss using Response Surface Methodology. However, the impact is expected to be minor, since the production manager has been altering the settings and registering the loss for many years. Regardless of the impact of this solution on the total loss reduction, it is still worthwhile to look into because it will not entail any increase in costs (CAPEX or OPEX) and is easy to implement. The only thing that has to be considered is that the optimal settings might reduce the feeder speed, resulting in a slightly lower production rate.

Pre-Grinding, score: 3.2
Another *primary* solution to reduce the heat production would be to minimise the blade speed since the two factors are non-linearly related (Figure 6.7). The only way to achieve a significant reduction in blade speed while maintaining the same final particle size is by reducing the input size to the grinder by pre-grinding the WIP into an (unknown) smaller particle size: DRAGxx. This way the required grinding power and the accompanying heat production is minimised per production step. The pre-grind step to DRAGxx and re-grind step to DRAG60 are shown graphically in Figure 6.11.

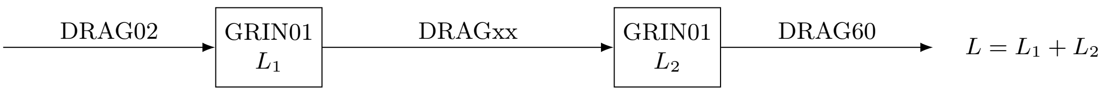

Figure 6.11: The regular DRAG60 production and the pre-grind option.

If such a pre-grinding step is used, the expectancy is that the accumulative loss of the pre-grind and re-grind step will be lower than for the single production step from DRAG02 to DRAG60. As for the other KPI's, the expectancy is that the operational costs for labour will increase for every production order since the total production time will double. Furthermore, by doubling the production time, the production rate will become twice as low, affecting the production planning significantly. Altogether the score for this solution becomes relatively low, but after discussing this option with management we concluded that it is still worthwhile to look into on an experimental basis since it is easy to test.

A second option for pre-grinding that was considered was to buy a so-called attrition mill to pre-grind the cinnamon to about 60-80% of its initial size. According to Reynolds Engineering & Equipment, this grinder works on the basis of cutting and shearing the cinnamon, creating almost no heat and loss during the process. However, even the highest size reduction of 80% would result in pieces of 4 mm at best. By looking at Figure 6.9 we can see that an input size of 4 mm has a minimal impact on the required grinding energy to re-grind it to DRAG60. This indicates that the involved energy during the re-grind process is will still be accompanied by high heat production, resulting in high production loss. It was therefore concluded that buying a second grinder to pre-grind is not a feasible option.

Inlet Cooling, score: 3.9
A *secondary* solution to minimise the production loss, is to lower the effective grinding temperature by drastically reducing the inlet temperature to the grinder. This way, the process will cool down internally by mixing it with cold air to ultimately reach a grinding temperature that is equal or lower than the ambient temperature, $T_{\text{grin}} \leq 32$ °C. This requirement is based on the fact that the lowest registered loss in GRIN02 is accompanied by grinding at a temperature that is close to the ambient temperature. Based on the plotted grinding temperature as a function of

the inlet temperature in Figure 6.6, the desired input temperature should be around $T_{\text{in}} = 5$°C. Furthermore, we know that the volumetric inflow of air should be $\phi_v = 1\ \text{m}^3/\text{s}$. To reach these two requirements, we need to look at temperature management systems in big buildings like offices and hotels. Most of these buildings are equipped with a so-called Air Handling Unit (AHU) in combination with a chiller, to regulate the temperature inside the building from one central point. The idea is to install such a cooling system onto the air inlets of the grinder, such that it cools down the process. In terms of performance for the different KPI's, the expectancy is that it will reduce the loss significantly while maintaining the production rate, but does come with additional capital and operational costs. Furthermore, it might take some time to install and calibrate the whole system, so a slightly negative effect on implementation. Based on the high score and discussion with management, it was again concluded that we could try this option but only if we could use the cooling system for a testing period, without immediately buying everything.

Cryogenic Process Cooling, score: 3.4
Cryogenic cooling works by cooling down the input material and grinding chamber to extreme lows, by adding liquid nitrogen to the process. This way, the grinding temperatures can be reduced to as much as -130 °C, drastically reducing the production loss due to the evaporation effect (Ghodki and Goswami, 2016). In the past, this solution was already considered, but after investigating the CAPEX and OPEX of this machine, management decided not go through with it. Their main concerns were the initial investment in a whole new grinding system (the current grinder is not compatible with this type of cooling) and the operational costs of cooling the process with liquid nitrogen. Based on these considerations, it was decided to not further look into this solution.

Material Cooling, score: 3.0
This solution focuses on cooling the input material before going into the grinding, as to slow down the evaporation effect during the process. This can be done by creating a cooled warehouse, or by cooling a specific batch before production (in the hopper for instance). An additional effect of cooling the warehouse is that the general warehouse loss of 1.2%s will also reduce. Management is however not convinced by this idea since they expect the impact to be minimal with respect to the required energy expenses for a cooled warehouse or hopper. Therefore, management indicated that they would only consider this option as some sort of additional solution to another process cooling solutions.

7 Candidate Solutions: In-Depth Effect and Cost Analysis

For this chapter, the focus will still be on the design cycle with a further analysis of the three most promising candidate solution. We will iterate between its construction and the evaluation, to eventually identify the final design (Hevner, 2007).

The in-depth analysis of the three picked candidate solutions will determine their expected effect on the loss reduction and whether the solutions are financially feasible in terms of the expected revenue increase compared to the involved costs. Please note that the loss reduction is calculated based on the average grinding loss of the past 2 months at 6.08% (compared to the yearly grinding loss of 6.23%).

7.1 Expected Revenue Increase

All candidate solutions aim at reducing the loss by minimising the evaporation effect, such that the cinnamon retains its moisture and volatile oil. This means that we increase the total output weight of the material which increases the revenue by \$6.75 per kilogram. Based on this information, the best way to estimate the revenue increase is by looking at the average cinnamon production over the last three years at a loss of 7.43%, and calculate what the production (and revenue) would have been for lower losses. However, one thing that needs to be considered when producing more output weight, is that the packaging cost increase by \$0.07 per produced kilogram (Tripper Nature, 2018). Therefore, Table 8 shows the (adjusted) revenue increase per percent loss reduction, by subtracting the packaging costs from the expected revenue increase. This increase of \$59,526 per percent loss reduction can now be used to determine the expected savings per candidate solutions by subtracting their accompanying costs from the revenue increase.

Please note that this amount is completely dependent on the yearly production and that the expected revenue increase is only true if the total production of 2018 is at least 825,000 kg. Therefore it can only function as an indication for further costs and savings calculation.

Table 8: Cost savings per reduced loss percentage, based on old data.

Loss (%)	Production (kg)	Revenue	Packaging costs	Revenue increase
7.4	825,165	\$5,569,869	\$-	\$-
6.4	834,076	\$5,630,018	\$623	\$59,526
5.4	842,987	\$5,690,168	\$1,247	\$119,052
4.4	851,898	\$5,750,318	\$1,871	\$178,578
3.4	860,810	\$5,810,468	\$2,495	\$238,104
2.4	869,721	\$5,870,617	\$3,118	\$297,630
1.4	878,632	\$5,930,767	\$3,742	\$357,156

7.2 Machine Settings Optimisation

The first candidate solution to analyse is to see if the current parameter settings of the grinder are actually optimal through the use of Response Surface Methodology.

7.2.1 Design of Experiment

For the design of experiment, the previously defined (coded) Design Matrix D for the Central Composite Design will be used where the first column represents factor A: the feeder speed (RPM), and the second column represents factor B: the blade speed (RPM). Since the coded variables correspond to the minimum and maximum actual values for both factors, they should to be determined first. The feed speed range is picked such that it stays within the ranges defined in Table 4. The range of the rotating speed of the beater plates must be determined by initial experimentation to check the lowest RPM possible while still meeting the granulation specification of DRAG60. The found minimum is 1550 RPM. Based on these ranges (and a small safety factor for the minimum blade speed), Table 9 shows the translation between these actual values to the coded variables to perform the thirteen experiments, where the loss induced by the grinder is registered as the the output response (so the warehouse loss is not included). The complete overview of the registered response is shown in Appendix D.

Table 9: The coded and actual ranges of the independent variables.

		Levels				
Factor	Variable	$-\sqrt{2}$	-1	0	1	$\sqrt{2}$
A	Feed speed (RPM)	28	30	35	40	42
B	Blade speed (RPM)	1580	1600	1650	1700	1720

7.2.2 Response surface and optimal settings

The Design Expert software package is able to analyse the registered data to create the response surface and find the optimal settings for minimal production loss. The relation between the feed speed, the blade speed and the loss is given in the quadratic (coded) equation

$$\text{Loss} = 5.84 + 0.20A + 0.51B + 0.15AB + 0.52A^2 + 0.27B^2 \tag{7.1}$$

and shown graphically in the 2D contour plot and the 3D surface plot. The equation reveals that there is a quadratic behaviour present for both factors and an interaction between the two factors (an AB term). An interesting thing to note is that the previously found increase of loss for low feeder speeds in Section 6.2.2, can also be identified in the two graphs below, although the surface response does to not exactly go through the actual value.

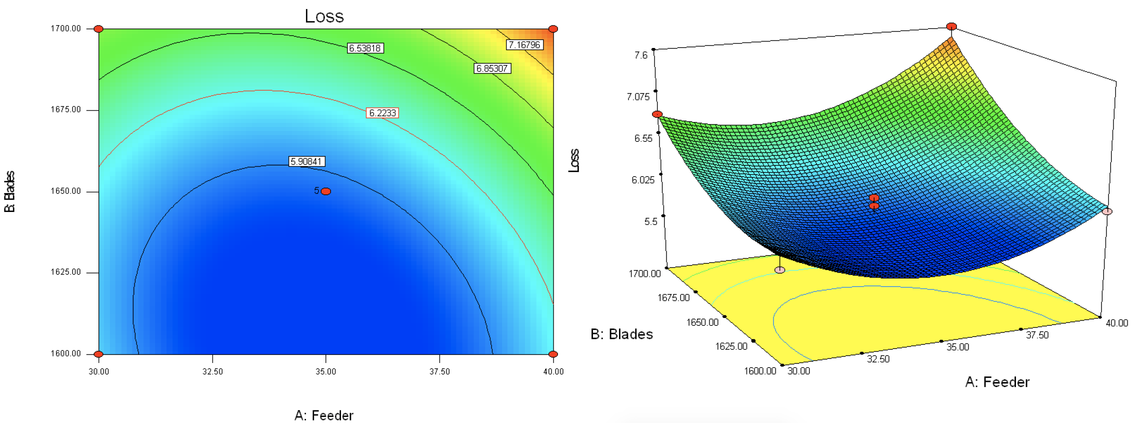

Figure 7.1: The contour plot and its 3D surface response.

According to the model, the minimum loss induced by the temperatures in the grinder is predicted to be 5.72% for the parameters denoted in Table 10.

Table 10: The required settings for minimal grinding loss.

A: Feeder (RPM)	B: Blades (RPM)	Response: Loss (%)
33.9	1590	5.72

7.2.3 ANOVA on RSM model

As introduced in Section 5, the regression model is analysed using the Fisher F-test with a 95% confidence interval and a probability value of [(Prob $> F$) < 0.05]. The fit of the model is checked by the determination coefficient R^2. The Analysis of Variance for the quadratic response surface model of the loss is shown in Table 11 with a F value of 40.02, $P \leq 0.05$ and a coefficient of determination of $R^2 = 0.9662$. This implies that the model is significant and that only 3.38% of the total variation is not explained by the model. This variation is shown in Figure 7.2 where the actual measured response of the experiment is compared to the predicted response of the model. It shows small variation, indicating that the fit and predictive capacity of the response surface is adequate. This is also represented in the acceptable difference between the value for the Pred R^2 (predicted) values and the Adj R^2 (adjusted) values. The relatively small variation is also supported by the given Coefficient of Variation ($CV = 0.75\%$).

Table 11: ANOVA for the response surface quadratic model of loss.

Source	Sum of Squares	df	Mean square	F-value	Prob $> F$
Model	**4.64**	**5**	**0.93**	**40.02**	**0.0001***
A	0.31	1	0.31	13.21	0.0083
B	2.10	1	2.10	90.47	0.0001
AB	0.90	1	0.09	3.88	0.0089
A^2	1.86	1	1.86	80.33	0.0001
B^2	0.50	1	0.50	21.46	0.0024
Std. Dev.	0.15		R^2	0.9662	
Mean	6.32		Adj R^2	0.9421	
C.V. %	0.75		Pred R^2	0.8428	

* Significant

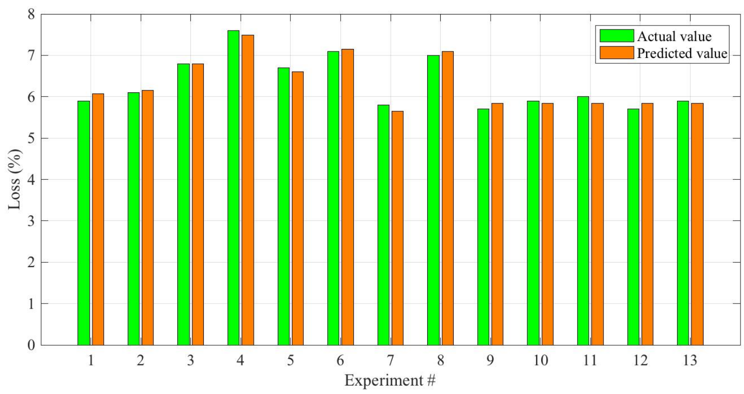

Figure 7.2: Difference between the actual and predicted values according to the created quadratic model.

7.2.4 Considerations for this solution

Altogether, it can be concluded that the model fits the response pretty well and has adequate predictive capabilities. Furthermore, the predicted loss for the ideal new machine settings gives a clear indication of what new settings could entail, and they also correspond to what we would expect based on our analysis of dynamics. If the predicted value for loss is true, Table 12 shows that the original production loss of 6.08% in the grinder can be reduced by 0.37% which results in yearly savings of $22,025, since there are no additional costs involved. However, one thing to consider is that the average production rate will decrease slightly as a result of lower feeder speed.

Table 12: Yearly financial benefit for using optimal machine settings.

Product	Reduction	Revenue	Costs	Savings
DRAG60	0.37%	$22,025	$0.00	$22,025

7.3 Pre-grinding

As concluded in Section 6.5, another *primary* solution to reduce the loss is by pre-grinding the material, to minimise the heat generation in the grinder during the production steps. The main issue here is to determine the ideal intermediate particle size of DRAGxx such that the heat generation per step is minimal. First, we determine this intermediate size theoretically, after which we perform small-scale experiments to check the effect on loss reduction.

7.3.1 The intermediate size of DRAGxx and its effect

Since we know that our initial particle size is always DRAG02 and the final size is always DRAG60, we need to find the optimal intermediate size for DRAGxx that requires the least amount of grinding power for the following two input-output pairs: DRAG02→DRAGxx and DRAGxx→DRAG60. This size can be determined by plotting the function of specific grinding power (Equation 6.6) for the two input-output pairs for varying output (x_2) and input (x_1) sizes. At the point where they intersect, the required grinding power (hence the RPM and heat production) is expected to be minimal for both steps. Figure 7.3 shows that the intersection is at 0.149 mm with a required grinding power of $P_{\text{grin}} = 9.0$ kW, making it similar to the DRAG50 production. Therefore, we will refer to this intermediate size as DRAG50*.

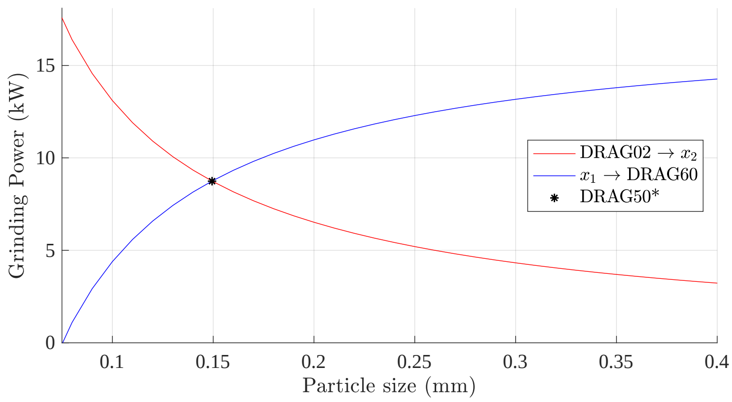

Figure 7.3: Point of intersect to show ideal intermediate particle size of DRAG50*.

The first thing to test is whether the grinding setting for DRAG50 will indeed be enough to pre-grind and re-grind to the eventual granulation size of DRAG60. Upon initial testing, the granulation specification for the #100 US mesh for DRAG60 (Table 1) was not met, unfortunately. The explanation could be found in the fact that in the re-grind step, the DRAG50* powder got sucked into the grinder more easily, reducing its total time in the grinding chamber, increasing the final granulation. However, after some more experimentation the required settings were found that met the granulation specifications for DRAG60. Figure 7.4 shows the resulting blade (B) and feeder (F) speeds in RPM for both steps, together with the grinding loss and the average accumulated loss for three experiments.

7.3.2 Considerations for this solution

The temperature per grinding step is significantly lower than for normal DRAG60 production, but the accumulated loss for both steps does not decrease, unfortunately. Furthermore, the volatile oil content in the cinnamon got below the threshold of 2.5%, so the quality specifications are not

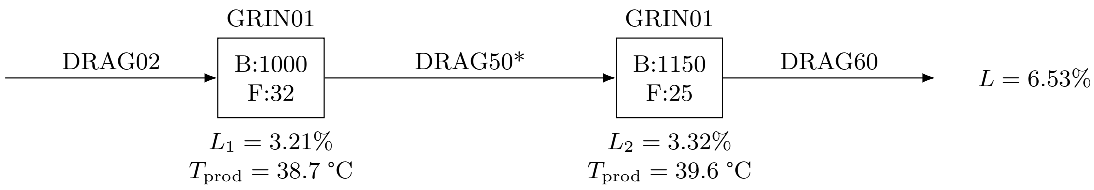

Figure 7.4: The settings and loss for both grinding steps, $N = 3$.

met either. The second concern with this option is that it intensifies the production planning significantly. The current average DRAG60 production time per day is around 3.2 hours, while the pre-grind step will increase this to 6.4 hours per day, increasing the yearly utilisation rate of GRIN01 from 54% to 94%. Altogether, it can be concluded that this solution does not appear to be effective.

7.4 Inlet Cooling

A third candidate solution to analyse is a *secondary* solution which aims at reducing the effective grinding temperature of the process by reducing the inlet temperature to the grinder. This way, the cold air will lower the grinding temperature such that the evaporation effect is minimised. As discussed in Section 6.5, the desired air input temperature should be around $T_{\text{in}} = 5$°C at a volumetric inflow of $\phi_v = 1$ m^3/s.

7.4.1 The Air Handling Unit (AHU) and Chiller

To meet the stated temperature and inflow requirements, the previously introduced inlet cooling system of an AHU and chiller is needed. Figure 7.5 shows a graphical layout of such a system. As can be seen, the system consists of two machines, the AHU on the left, and the water chiller on the right. The systems 'interact' with each other through the coil evaporators. In Appendix E, the working principle of the two systems is explained in more detail.

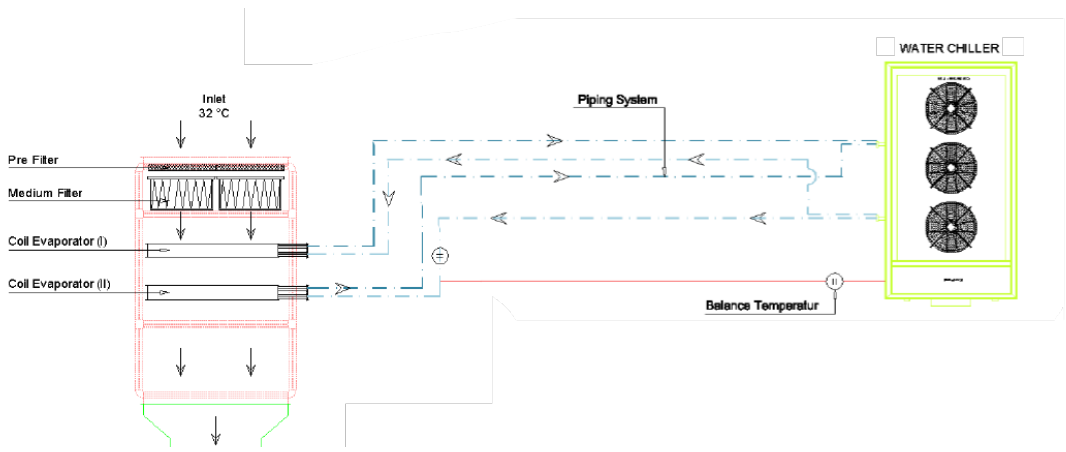

Figure 7.5: Graphical layout of the chiller and AHU (Surya Marga Luhur, 2018).

Vendor Proposal

After contacting several vendors with the request to deliver the required cooling system, only one vendor came through with a proposal. According to their calculations, we need a chiller with a capacity of 500,000 BTU and an AHU of 350,000 BTU at 3500 CFM. Furthermore, the vendor offered two options: a monthly rental plan including service, or to just buy the whole system. We decided to rent the cooling system for two months, such that we could conduct experiments with it to determine the impact on the loss reduction.

7.4.2 Effect of inlet cooling system

After the vendor installed the complete cooling system onto the air inlets of the GRIN01 (see Appendix F), we conducted initial experiments on DRAG60 and DRAG50 production. Upon initial running of the cooling system, we found that it was not able to reach the theoretical temperature of $T_{\text{in}} = 5°\text{C}$, but operated at $T_{\text{in}} = 14°\text{C}$. This results in a theoretical grinding temperature of 40°C for DRAG60, so the requirement of $T_{\text{prod}} \leq 32$ °C could not be reached. Therefore, we also experimented with DRAG50 production, since we expected its grinding temperatures to be lower than 30°C and it would be interesting to see the loss for these temperatures. Table 13 shows the average loss over 6 trials for DRAG60 and 4 trials for DRAG50 and its reduction with respect to its normal grinding loss.

Table 13: The results for initial experiments with the inlet cooling system in place.

Experiment	Temperature (°C)	Grinding loss (%)	Reduction (%)
DRAG60$_{N=10}$	42	4.51	1.57
DRAG50$_{N=6}$	22	1.39	1.87

7.4.3 Considerations for this solution

The use of the inlet cooling system yields a loss reduction of 1.57% for DRAG60 and a 1.87% loss reduction for DRAG50. Since this cooling system reduces the loss of both products, the total revenue increase from Table 8 should be adjusted for the additional revenue from DRAG50 production at \$10,503 per percent loss reduction (Tripper Nature, 2018). Table 14 shows this yearly revenue increase for both products, with a total of \$113,096. However, this solution also comes with higher capital and operational expenses. To calculate the resulting savings of this measure, we need to determine these capital and operational costs first. Since the vendor offered both a rental and buy option, Appendix G gives a complete overview of the yearly costs per option of \$16,463 and \$15,742 respectively. Due to the short depreciation period of the chiller and the possible required service, management only considers the rental plan for future use. When using the rental option, we know that the cost for operating the inlet cooling system is equal to \$13.07/h, resulting in yearly costs of \$16,642. The yearly savings created by using the inlet cooling system comes down to \$96,454.

Table 14: Yearly financial benefit for using inlet cooling system.

Product	Reduction	Revenue	Costs	Savings
DRAG60	1.57%	\$93,456	\$13,465	\$79,990
DRAG50	1.87%	\$19,641	\$3,177	\$16,464
	Total	\$113,096	\$16,642	\$96,454

7.5 Inlet Cooling with Optimal Settings

A logical follow-up on the inlet cooling solution would be to check if we can find new optimal settings for the cooled grinder. The expectancy is that the dynamics of cooled DRAG60 production is different from normal DRAG60 production, especially the impact of the feeder speed discussed in Section 6.2.2.

7.5.1 Design of Experiment

In order to check this, a new RSM analysis is performed on the system with identical ranges for the coded and actual values as in Table 9, corresponding to the solutions design matrix D of the Central Composite Design. The response for all thirteen experiments can be found in Appendix H.

7.5.2 Optimal Settings with Inlet Cooling

The analysis of the response using the Design Expert software package relates the factors to the response through the following polynomial

$$\text{Loss} = 4.38 + 0.24A + 0.41B - 0.18AB + 0.23B^2. \tag{7.2}$$

Note that this polynomial does not contain the A^2 term anymore, indicating that the relationship between loss and the feeder speed is now expected to be linear. Furthermore, when looking at the contour and surface plot in Figure 7.6, we can see that the minimal loss got shifted more into the corner for lower feeder and blade speeds. According to the response surface, the lowest loss of 3.89% can be achieved for the settings in Table 15. Based on our own knowledge on the grinder dynamics, this seems like a logical configuration since it minimises the turbulence due to the blade speed and the dissipation of heat during breaking by limiting the volumetric inflow of cinnamon.

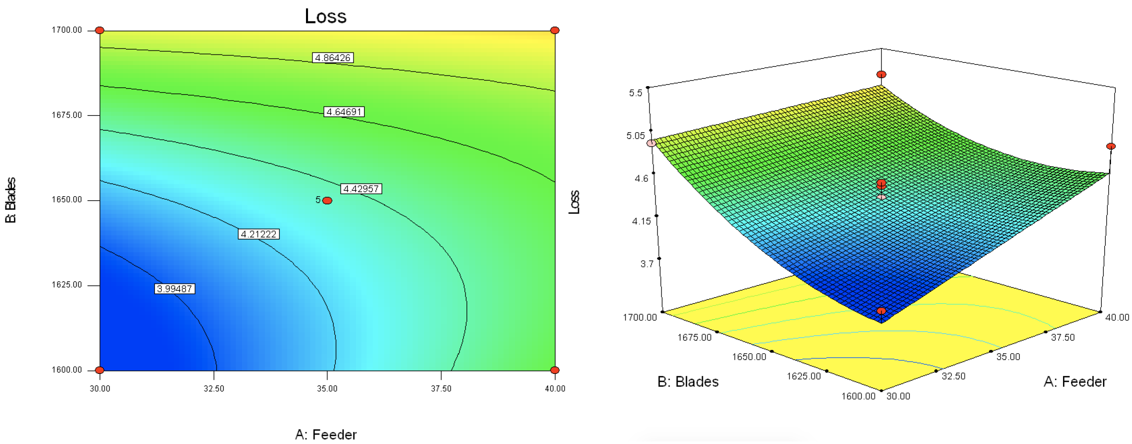

Figure 7.6: The contour plot and its 3D surface response.

Table 15: The required settings for minimal grinding loss.

A: Feeder (RPM)	B: Blades (RPM)	Response: Loss (%)
31	1580	3.89

7.5.3 ANOVA on RSM model

Table 16 shows the summary of the Analysis of Variance for the quadratic response surface model. The model appears to be significant with a F value of 15.61, $P \leq 0.05$ and a coefficient of determination of $R^2 = 0.8864$, hence, the model is significant, and only 11.3% of the total variation is not explained by the model. The variation between the actual response and the predicted response for the different experiments can be found in Figure 7.7, which shows more variation than for the previous model. Furthermore, the difference between the Pred R^2 and the Adj R^2, indicates that the predictive capabilities of this model are less accurate. Therefore, the found optimal settings and its corresponding predicted loss should be taken with some discretion.

7.5.4 Considerations for this solution

The expected grinding loss for DRAG60 using inlet cooling and optimal settings becomes 3.89%, while for DRAG50 it will stay the same at 1.87%. This means that we can gain additional savings compared to using the inlet cooling system only, shown in Table 17. The increase of yearly savings is equal to $36,906, while the costs will stay the same. However, keep in mind that this estimation is based on a model with moderate predictive capabilities, so the real loss reduction might differ.

Table 16: ANOVA for the response surface quadratic model of loss.

Source	Sum of Squares	df	Mean square	F-value	Prob > F
Model	**2.34**	**4**	**0.58**	**15.61**	**0.0008***
A	0.46	1	0.46	12.31	0.0080
B	1.36	1	1.36	36.26	0.0003
AB	0.13	1	0.13	3.56	0.0960
B^2	0.39	1	0.39	10.29	0.0125
Std. Dev.	0.19		R^2	0.8864	
Mean	4.52		Adj R^2	0.8296	
C.V. %	4.28		Pred R^2	0.5381	

* Significant

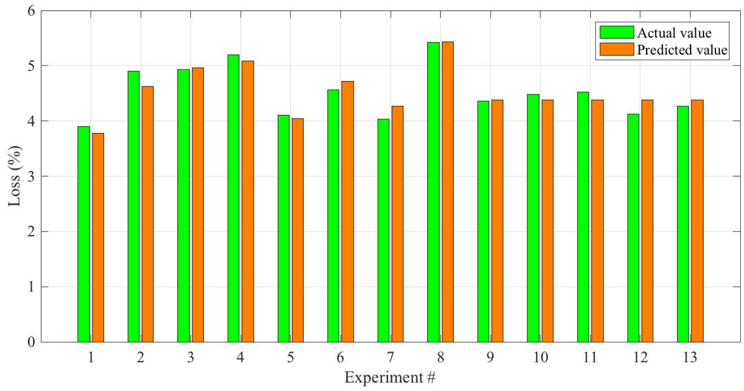

Figure 7.7: Difference between the actual and predicted values according to the created quadratic model.

Table 17: Yearly financial benefit for using inlet cooling system with optimal grinding settings.

Product	Reduction	Revenue	Costs	Savings
DRAG60	-2.19%	\$130,362	\$13,468	\$116,894
DRAG50	-1.87%	\$19,641	\$3,177	\$16,463
	Total	\$150,003	\$16,646	\$133,357

7.6 Inlet Cooling during Pre-Grinding

The results from the previous sections show us an interesting relationship between the pre-grind and inlet cooling experiments, that might indicate the possibility to even further reduce the production loss. By using the fact that the ideal intermediate step size of DRAG50* is similar to DRAG50, and the losses for the pre-grind and re-grind step were similar to normal DRAG50 production, we could conclude that by using the cooling system in combination with the pre-grind solution, the production loss per step will also be equal to about 1.4% (based on Table 13). This might result in an accumulated loss of about 2.8%, which is even lower than DRAG60 production with inlet cooling and optimal settings. To test this hypothesis, six experiments were conducted for the pre-grind solution in combination with the inlet cooling system, with the average results shown in Figure 7.8, where all quality specification are met.

7.6.1 Considerations for this solution

The accumulated loss of both steps is equal to 3.09%, which yields a total loss reduction of 2.99% for DRAG60. As given in Table 18, this loss reduction in combination with the previously found

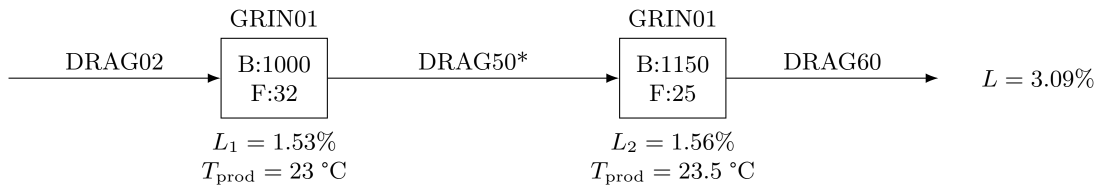

Figure 7.8: The pre-grind option in combination with the inlet cooling system.

loss reduction for DRAG50 while using the inlet cooling, results in a total increase in yearly revenue of $197,624. Now to calculate the actual savings, Appendix I gives an overview of the additional yearly costs of pre-grinding at $9,260. This amount has to be added to the yearly costs of operating the inlet cooling system, resulting in yearly costs of $25,902.

As discussed before, the only downside of pre-grinding will be the fact that the production rate reduces to 400 kg/h. The consideration that has to be made here is whether it is possible and worth to save more money, at the costs of a lower production rate.

Table 18: Yearly financial benefit for using inlet cooling system during pre-grinding.

Product	Reduction (%)	Revenue	Costs	Savings
DRAG60	2.99	$177,983	$22,725	$155,257
DRAG50	1.87	$19,641	$3,177	$16,464
	Total	$197,624	$25,902	$171,721

7.7 Solutions Overview and Implemented Solution

To conclude this chapter, a quick overview of all the solutions, their effect and yearly savings are given, followed by a short description of the decision process towards the implemented solution.

7.7.1 Solution overview

Figure 7.9 gives an overview of the expected yearly savings (green), based on the difference between additional revenue (cyan) and additional costs (orange) for each candidate solution.

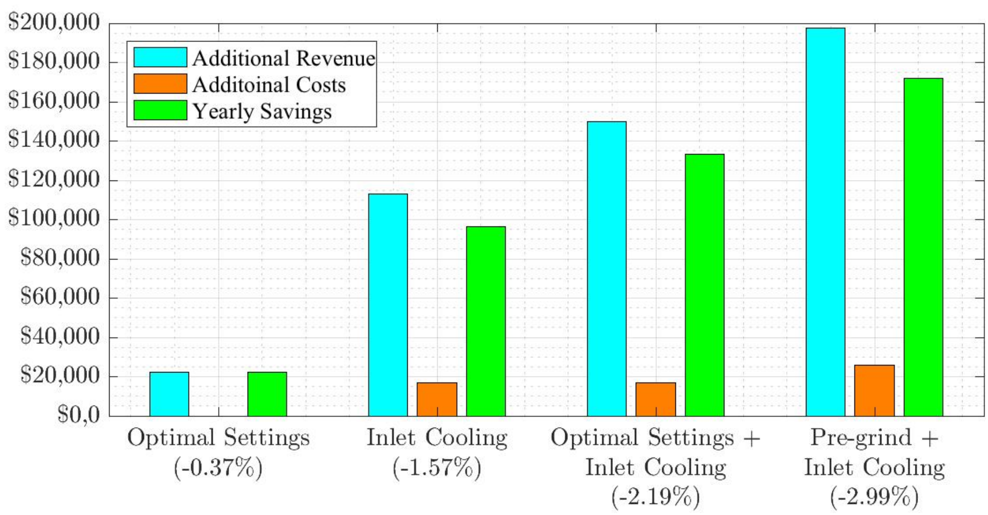

Figure 7.9: Overview on the resulting savings per candidate solution.

The overview clearly shows that the highest loss reduction and savings can be achieved by pre-grind the cinnamon while using the inlet cooling system. It yields a reduction of 2.99% resulting in yearly savings of $171,721, which is a considerable amount of money. However, this option does come with the 'cost' of a reduced production rate and an increase in machine utilisation. Since the production rate is something that management considers as important, it is up to them to determine if they see this option as viable. The second best option, where the inlet cooling system is used with optimal settings, also shows promising results. In the case where management is not willing to intensify their production planning, this option is still able to reduce the production loss for both DRAG60 and DRAG50 significantly, resulting in yearly savings of $133,357. The last two options of using only inlet cooling or optimal settings become obsolete with respect to the previous two.

7.7.2 Implemented Solution

In order for the management team to make a decision on the best solution to implement, we created a new solutions design matrix, containing the above-analysed candidate solutions. Based on the experiments and predicted loss reductions, Table 19 shows the new scores per candidate solution, constructed in collaboration with the management team.

Table 19: The new weighted solutions design matrix for the analysed candidate solutions.

	L	C	P	I	
Weight	0.4	0.3	0.2	0.1	Score
Optimal machine settings	1	5	4	5	2.8
Inlet cooling	3	3	5	5	3.1
Inlet cooling + optimal settings	4	3	4	5	3.4
Pre-grinding + inlet cooling	5	2	2	1	2.9

L	Loss reduction
C	Cost minimisation
P	Production rate
I	Implementation

It clearly shows that although the pre-grind option with inlet cooling scores very high on the loss reduction, they were not pleased with the resulting production rate and the fact that it intensifies the complete planning. In addition, we came to the conclusion that having a lower production rate and DRAG50* as an additional product in the warehouse, the implementation of this solution is harder than expected. Therefore, this candidate solution only scores a 2.9. The solution that they graded the best, was the inlet cooling in combination with the optimal settings. Based on the fact that the complete system was already installed for the experimentation period, they concluded that apart from the additional costs, this solution scores best. The only minor downside is that by using the optimal settings from the RSM analysis, the production rate will drop. However, they mentioned that they will try to use it anyways, but might increase the feeder speed in the future.

So, based on the discussions and the final solutions design matrix, management chose to use the inlet cooling system in combination with the optimal settings immediately, resulting in expected yearly savings of about $133,357. In the next chapter, the solution will be evaluated and these predictions on loss reduction will be verified by looking at the data from large-scale production data of DRAG60 and DRAG50 of one month, using the implemented solution.

8 Evaluation of Implemented Solution and Conclusion

In accordance with Hevner's design cycle, the very last step is to thoroughly evaluate the final design. For this research, the evaluation consists of two parts: verification and validation. The first part is to verify whether the expected loss reduction from the (small-scale) experiments actually correspond to the real loss reduction when the solution is used in daily production. In case of differences in results, the rigor and relevance cycle can be used to find explanations for it. The second part consists of validating the final design with respect to the stakeholder requirements.

8.1 Verification of Loss Reduction

Since the expected loss reduction for the implemented solution is based on small-scale experiments, it is interesting to verify whether the impact of the implemented solution is actually the same for large-scale production. To verify, we can use the production data from September - October and determine the real impact of the inlet cooling system with optimal settings. These results indicate if the experiments were indeed representative and whether the predicted losses of the Response Surface Methodology are actually true. In Table 20 and Table 21 the complete production scheme is given for both DRAG60 and DRAG50, together with their losses. Keep in mind that the registered production loss in the database of Tripper Nature also includes the warehouse loss. Furthermore, the production manager informed us that the used settings for DRAG60 were 1575 RPM for the blade speed and 32 RPM for the feeder speed, which is slightly different from the found optimal settings from the RSM analysis. He stated that he increased the feeder speed such that the production rate would still be acceptable, with an average of 763 kg/h.

Table 20: DRAG60 production data from the period 04/09 - 02/10 (including warehouse loss).

Product	Date	Input (kg)	Output (kg)	Loss (%)
DRAG60	Sep 10 2018	800	772	3.37%
	Sep 13 2018	1,200	1,157	3.58%
	Sep 27 2018	3,348	3,298	1.49%
	Sep 28 2018	1,430	1,407	1.61%
	Oct 01 2018	4,845	4,741	2.15%
	Oct 02 2018	5,074	4,964	2.17%
	Total	16,697	16,340	2.14%

Table 21: DRAG50 production data from the period 04/09 - 02/10 (including warehouse loss).

Product	Date	Input (kg)	Output (kg)	Loss (%)
DRAG50	Sept 04 2018	1,782	1,750	1.57%
	Sept 05 2018	3,380	3,325	1.33%
	Sept 06 2018	4,713	4,635	1.44%
	Sept 07 2018	4,198	4,170	1.24%
	Sept 10 2018	2,349	2,319	1.28%
	Total	16,422	16,199	1.36%

The results show that for the DRAG60 production, the average production loss equals 2.14%. Compared to the average production loss of the last two months of 7.28% (including warehouse loss), this yields a total loss reduction of 5.14%. The DRAG50 production loss averages out at 1.36%, also including warehouse loss. This means that the total loss reduction for DRAG50 is equal to 3.10%. Table 22 gives the summary of these loss reductions and their expected yearly financial benefit for Tripper Nature. The complete yearly savings as a result of this solution adds up to $321,881.

Table 22: Yearly financial benefit using inlet cooling system with optimal grinding settings.

Product	Reduction	Revenue	Costs	Savings
DRAG60	5.14%	$305,964	$13,465	$292,498
DRAG50	3.10%	$32,559	$3,177	$29,383
	Total	$338,523	$16,642	$321,881

8.1.1 Explanation for the difference in predicted and real loss reduction

From this verification, it becomes clear that there is a significant difference between the expected loss reduction from the small-scale experiments and the real loss reduction from large-scale production, summarised in Table 23. Although the difference is in favour of Tripper Nature, it is still important to find an explanation for it.

Table 23: Differce between expected loss reducuction and real loss reduction.

Product	Expected	Real	Difference
DRAG60	2.19%	5.14%	2.95%
DRAG50	1.87%	3.10%	1.23%

The following aspects could explain this difference where the first applies to the difference of both products, while the second explanation only applies to DRAG60.

General variance in production loss

Throughout the period of this research and analysis of old data, something that came to light is that there is a significant variance in production loss. For DRAG60 and DRAG50, the found average of 7.43% and 4.46% are accompanied by a standard deviation of 1.14% and 0.62% respectively. This variation can be explained by variance in warehouse loss, which is dependent on the storage time of WIP, and the (seasonal) variances in the initial moisture content of the cinnamon. According to Jung et al. (2018) and Barnwal et al. (2014b), the moisture content of cinnamon has some effect on the properties of the material in terms of brittleness and heat diffusivity. Higher moisture content results in a tougher material that requires more energy to break down, in combination with an increase in thermal diffusivity. This would suggest that theoretically speaking, cinnamon with higher initial moisture content will result in slightly higher production loss due to evaporation since more (heat) energy is involved during the process, in combination with higher heat diffusivity of the cinnamon. Furthermore, the cinnamon business manager confirmed that there is indeed a seasonal variance in initial moisture content of the cinnamon, but that some of the farmers in Sumatra also mist the cinnamon bars with water a few days before transport to Jakarta, as to increase the moisture content and the total weight of the product.

Predictive capabilities of RSM analysis

This explanation only applies for the difference in expected and real loss reduction for the DRAG60, since that is where we used RSM analysis to find optimal settings, together with its expected loss. From the ANOVA on the model, we already concluded that the predictive capabilities of the model were limited and that we should take the prediction with some discretion. Since the found difference for DRAG60 is significantly higher than for DRAG50, it is plausible that the predicted loss reduction of the RSM model was indeed too low.

8.2 Validation of Implemented Solution

In a broader sense, it is of importance to determine whether we resolved the stated problem and reached our research and design goal through the implementation of the solution while meeting the stakeholder requirements constructed in the beginning of this research.

8.2.1 Problem and goal validation

The main problem consisted of the evaporation effect of moisture and volatile oil, resulting in production loss, residue forming (leading to downtime) and lower product quality. The goal was therefore to find the best way to minimise this evaporation effect and implement the solution into the production line.

After running the eventual solution during daily production, it became apparent the evaporation effect drastically decreased, reducing the production loss, but also the residue forming in the piping after the grinder. The production engineer informed us that since the installation of the inlet cooling system, no oily substance has been dripping from the exhaust pipe. This indicates that the buildup of residue in the piping after the grinder has decreased, possibly reducing the downtime due to cleaning and replacing of the dust collectors. As for the product quality, we would expect that it will also increase since less volatile oil evaporates from the cinnamon. However, we are only able to determine this after a full year of production to see if the average content of volatile oil of DRAG60 increased compared to last year, to minimise the seasonal variances.

8.2.2 Stakeholder requirements validation

As for the stakeholder requirements, Table 24 shows the complete overview per stakeholder and whether the implemented solution meets them. Below, the validation is explained in more detail per stakeholder.

Table 24: Validation of stakeholder requirements.

Stakeholder	Requirement for solutions	Quantification	Results
Cinnamon business manager	Reduce the production loss for DRAG60	-5%	-5.14%
	Meet granulation specifications	Table 1	OK
	Minimum volatile oil content	2.5%	OK
	Minimum moisture content	7.5%	OK
	Financial feasibility	-	OK
Production manager	No interference with production	-	OK
	Planning feasibility	-	OK
	Average production rate of DRAG60	≥800 kg/h	763 kg/h
Production engineer	Settings should stay within range	Table 4	OK
	Implementation feasibility	-	OK
Operators	-		

Cinnamon business manager

The main requirement (and goal) stated by the business manager was to reduce the total production loss for DRAG60, preferably by 5%, such that it would resemble the losses of the other cinnamon products. Although this requirement did not seem to be met during the small-scale experiments of the solution, it did have the additional advantage that it also reduces the production loss for DRAG50. Due to this additional benefit, its financial feasibility and the fact that the quality specifications (granulation, moisture and volatile oil) were met, the cinnamon business manager decided to implement it anyways. Upon verifying whether the expected loss reduction corresponded to the real loss reduction, we found that there is a significant difference between them, resulting in a loss reduction that even meets the initial requirement of 5% reduction. However, it is important to mention that this can be temporary, because of the previously explained variance in production loss that occurs. The only way to really know the impact is to monitor the results for a longer period of time.

Production manager

The only requirement that is not met with the currently implemented solution is the required production rate of 800 kg/h, since the new settings for DRAG60 production entail a small reduction of about 40 kg/h. As mentioned before, the production manager already decided to increase the feeder speed from the initially found 31 RPM to 32 RPM, as to minimise the production rate decrease and impact on the planning. As for the interference of the experiments with regular production, no real issues were encountered. Furthermore, a possible breakdown of the inlet cooling system does not interfere with production in general, only the loss will increase again.

Production engineer
The last two requirements came from the production engineer where the new settings are still within the range of the machine, and the implementation requirement was met easily. It took the vendor only two days to fully install the chiller and air handling unit onto the grinder, and in case of breakdowns, the vendor is responsible for the repair.

Operators
Although the operators did not have any requirements for this research, they are slightly impacted by the eventual solution, since they now also have to operate the inlet cooling system. However, this only consists of flipping some switches 15 minutes prior to production such that the chiller is operating at the required temperature.

8.3 Conclusion

The goal of this research was to identify and implement a way to reduce the production loss of 7.43% for DRAG60 cinnamon in grinder GRIN01. Initial investigation on the true cause of the production loss showed that high temperatures of 57.2°C during the grinding process, cause the moisture and volatile oil in the cinnamon to evaporate, decreasing their weight based content which results in direct weight loss of the output. These high grinding temperatures appeared to be the result of heat production in the grinder as an effect of three main factors: 1) turbulence inside the grinder created between the rotating blades and the corrugated lining; 2) dissipated heat during the actual breaking of the cinnamon, and 3) the air inlet temperature to the grinder which is relatively high in Jakarta. By decreasing the impact of these three factors, the effective grinding temperature in GRIN01 reduces, minimising the evaporation effect of moisture and volatile oil resulting in lower weight loss of the cinnamon.

Based on to these factors, a total of five candidate solutions were identified, of which three were picked by management for further analysis: 1) see if the current settings for grinding DRAG60 are actually optimised for the lowest production loss, 2) reduce the particle input size for GRIN01 through pre-grinding the cinnamon, such that minimal grinding power is required, reducing its equivalent heat production and 3) lower the inlet air temperature to GRIN01, as to cool down the complete grinding process.

After the in-depth analysis of their impact and costs and weighing them against the stakeholder requirements, we found that the most suitable solution would be to combine some of the solutions. The eventual implemented solution was to grind DRAG60 using optimal settings (and regular DRAG50 production) in combination with the inlet cooling system. After implementation of the solution and large-scale production during September and October, the loss reduction yielded 5.14% for DRAG60 and a reduction of 3.10% for DRAG50. Based on these loss reductions, their added revenue and accompanying costs, the actual yearly savings come down to $321,881. Furthermore, the implemented solution meets all but one stakeholder requirement: the current production rate of 763 kg/h is too low compared to the required 800 kg/h.

8.4 Discussion

Apart from the already discussed discrepancy between the predicted and real loss reduction following the implemented solution, there are a few other things that are worth mentioning.

With the current implemented solution, the total production loss in GRIN01 is decreased significantly, while meeting most stakeholder requirements. The only stakeholder requirement that is not completely met, unfortunately, is the minimal production rate of 800 kg/h. However, while discussing the candidate solutions and their effect with management, they concluded that although it is an important requirement, there is some room for flexibility. They stated that if a decrease in production loss can be achieved with such a relatively easy measure, they regard is as a necessary sacrifice.

Second, it is important to note that all calculations performed on the dynamics of the system only give an indication of their real values. So for the power flow diagram in Figure 6.10, the calculated values can only be used as an order of magnitude. The uncertainty mainly lies in the amount of dissipated heat due to breaking, since its energy was measured by the increase in airflow temperature coming from the grinder. However, this amount of energy that was used to heat up the air is not equal to the total amount of energy created due to breaking, since the biggest part of it will be absorbed by the cinnamon particles themselves. Furthermore, air is a terrible conductor of heat, so the expectancy is that in reality, the impact of this dissipated energy is higher than calculated. However, regardless of this uncertainty, the calculations on the power flow could be used to at least give us some insight into the dynamics of the system and point us towards possible candidate solutions.

A third finding that remains partly unexplained, is the behaviour of loss as a result of low feeder speeds in case of normal DRAG60 production. What we know is that the evaporation effect in the grinder increases when the feeder speed increases, due to the higher volumetric inflow that dictates the dissipated energy from breaking. The interesting thing is, that for very low feeder speeds of 25 RPM, the loss did not appear to be the lowest. The only reason that we could come up with, was that for these low feeder speeds, the number of cinnamon particles in the grinder is less, thus increasing the heat absorption (generated by the turbulence) per particle. However, we were unable to fully prove this theory. The only thing that was noted, is that when the inlet cooling system was put into place, this increase of loss for low feeder speeds did not appear.

The last thing to note is the fact that for the pre-grind experiments, the complete output of DRAG50* from the first step, was inserted back into the hopper for the re-grind step. Something that was not taken into account in this case, was that some part of the cinnamon coming out of the pre-grind step, actually already meets the granulation requirements for DRAG60. It would therefore not be necessary to re-grind this material again, exposing it to the heat in the grinder.

8.5 Future Extensions

During the problem analysis it became clear that apart from the loss induced by the grinder, the cinnamon also loses 1.2% of its weight while it is in storage as work-in-process material. This weight loss can also be attributed to the evaporation of moisture and volatile oil, although at much lower rates. It might, therefore, be interesting to look into this problem. A solution could be to cool down the warehouse, as to minimise the evaporation effect. Another option would be to minimise the time that the WIP material is stored in the warehouse.

A second thing that could be considered, is to check whether DRAG50 is actually produced at the lowest blades speeds possible. Based on the fact that Tripper Nature produced DRAG60 way above its own granulation standards that enabled them to produce at lower speeds, might indicate that the same thing goes for DRAG50 production. This could entail even lower losses for DRAG50 when combined with the inlet cooling system.

A third extension would be to see if the pre-grind option can be optimised, such that it produces at the desired production rate. Since Tripper Nature is planning on redesigning the complete production process after GRIN01, there might be possibilities to see if they can achieve a continues production line, where they produce at lower blade speeds, sift all the material, and automatically re-direct the cinnamon that does not meet the DRAG60 granulation specification back into the hopper. This way they minimise the heat production in GRIN01 and in combination with the inlet cooling system yield interesting results.

References

Alvarez, L. (2000). Design optimization based on genetic programming. *University of Bradford, UK.*

Barnwal, P., Mohite, A., Singh, K., Kumar, P., Zachariah, T., and Saxena, S. (2014a). Effect of cryogenic and ambient grinding on grinding characteristics of cinnamon and turmeric. *International J. Seed Spices*, 4(2):26–31.

Barnwal, P., Singh, K., Mohite, A., Sharma, A., and Zachariah, T. (2014b). Determination of thermal properties of cryo-ground cinnamon powder. *Journal of Spices and Aromatic Crops*, 23(2):262–267.

Davim, J. P. and Aveiro, P. (2016). *Design of experiments in production engineering.* Springer.

den Akker, V. and Mudde, R. F. (2014). *Transport phenomena: the art of balancing.* Delft Academic Press.

Fan, Y., Lu, W., Zhou, Y., Yan, P., Leng, Z., and Chen, M. (2016). Influence of tunneling methods on the strainburst characteristics during the excavation of deep rock masses. *Engineering Geology*, 201:85–95.

Freeman, R. E. (2010). *Strategic management: A stakeholder approach.* Cambridge university press.

Ghodki, B. M. and Goswami, T. (2016). Optimization of cryogenic grinding process for cassia (cinnamomum loureirii nees l.). *Journal of food process engineering*, 39(6):659–675.

Hevner, A. R. (2007). A three cycle view of design science research. *Scandinavian journal of information systems*, 19(2):4.

Jung, H., Lee, Y., and Yoon, W. (2018). Effect of moisture content on the grinding process and powder properties in food: A review. *Processes*, 6(6):69.

Khuri, A. I. and Mukhopadhyay, S. (2010). Response surface methodology. *Wiley Interdisciplinary Reviews: Computational Statistics*, 2(2):128–149.

Moran, M. J., Shapiro, H. N., Boettner, D. D., and Bailey, M. B. (2010). *Fundamentals of engineering thermodynamics.* John Wiley & Sons.

Morshedi, A. and Akbarian, M. (2014). Application of response surface methodology: design of experiments and optimization: a mini review. *J Fund Appl Life Sci*, 54:2434–9.

Murthy, C. and Bhattacharya, S. (2008). Cryogenic grinding of black pepper. *Journal of Food Engineering*, 85(1):18–28.

Rahman, S. and Ahmed, J. (2012). *Handbook of food process design.* John Wiley & Sons.

Ravindran, P., Nirmal-Babu, K., and Shylaja, M. (2003). *Cinnamon and cassia: the genus Cinnamomum.* CRC press.

Reynolds Engineering & Equipment (2001). Installation, Operation and Maintenance Instruction for Air Swept Pulveriser Model 28-H. Hard copy.

Saravacos, G. D., Kostaropoulos, A. E., et al. (2002). *Handbook of food processing equipment.* Springer.

Singh, K. and Goswami, T. (1999). Design of a cryogenic grinding system for spices. *Journal of Food Engineering*, 39(4):359–368.

Surya Marga Luhur (2018). Quotation and graphical layout of AHU + Chiller. Hard copy.

Tripper Nature (2018). Internal documentation on operational expenditures of GRIN01. Excel sheet.

Ullmann, F., Gerhartz, W., Yamamoto, Y. S., Campbell, F. T., Pfefferkorn, R., Rounsaville, J. F., et al. (1985). *Ullmann's encyclopedia of industrial chemistry.* VCH publishers.

Appendices

A Cinnamon Supply Chain

The supply chain of Cassia cinnamon, depicted in the figure below, starts at a cinnamon tree plantation in West Sumatra. This is where the Cassia cinnamon trees are grown to sufficient size in an average period of 25 years. The supplier has two ways of obtaining the cinnamon, either by buying about one hectare of a cinnamon plantation and harvest themselves, or by buying the harvested cinnamon from farmers and collectors. In case of buying the plantation, they will inspect whether the trees are ready to harvest by checking the leaves. If there are too many young (red) leaves on the tree, the harvesting should be postponed, because the cinnamon tree bark is too sticky to peel from the trunk. In case there are no more red leaves on the tree, initial trunk peeling can start. In this step, the first 30 cm of the bark from the ground up will be removed to kill the tree in the upcoming month. After one month, the tree will be chopped down, the bark will be peeled, cleaned and left to dry. It takes up to one month to harvest one hectare of cinnamon, which produces between 30-40 tons of dried cinnamon bark. The harvested cinnamon by the supplier and farmers is stored in the supplier's warehouse in Sumatra, after which it can be transported to Tripper Nature in Jakarta by truck and boat.

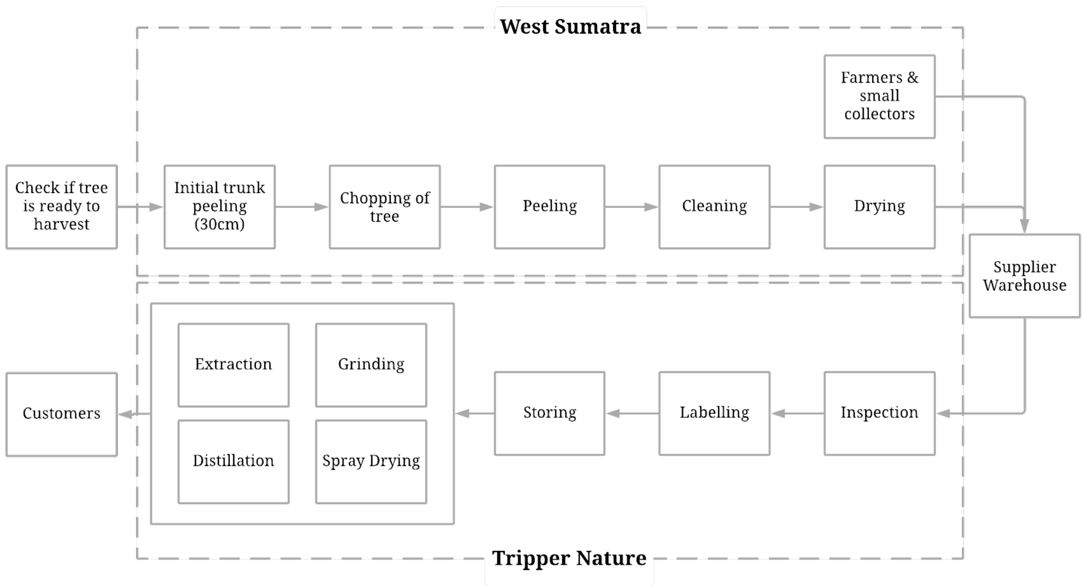

Cinnamon Supply Chain Schematic.

At Tripper Nature, cinnamon arrives as dried cinnamon bars in plastic nets. All the nets are inspected for irregularities after which they are labelled and stored in so-called intainers. These intainers have a removable bar in the middle to make the (un)loading process easier. Furthermore, they can be stacked vertically such that they become the storage racks in the warehouse. The last step before shipping the product to the customer is the Added Value Process of Tripper Nature. The value is added by either grinding, extracting, distilling or spray drying the cinnamon.

B The Product Collector

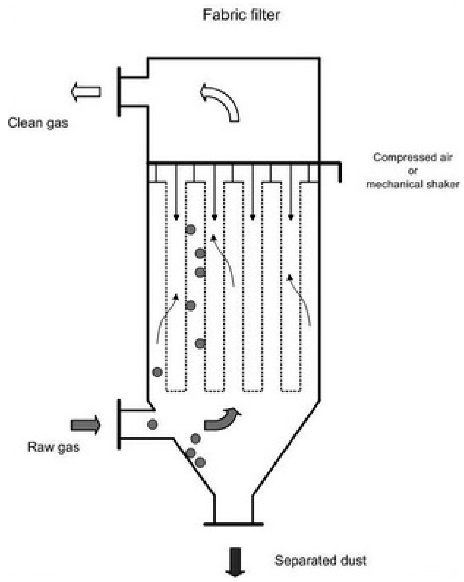

Product collector with cylindrical dust collectors.

C GRIN01 in standard condition

Here the standard situation for GRIN01 is shown where the ambient air gets sucked into the GRIN01 at two different air inlets (I and II). Air inlet I sucks the air in at a rate of $\phi_{\mathrm{v,I}} = 0.8\ \mathrm{m}^3/\mathrm{s}$, while air inlet II, close to the feeder system, has an inflow of $\phi_{\mathrm{v,II}} = 0.2\ \mathrm{m}^3/\mathrm{s}$. The total inflow therefore becomes $\phi_{\mathrm{v}} = 1.0\ \mathrm{m}^3/\mathrm{s}$ which is equal to the outflow indicated by the red arrow.

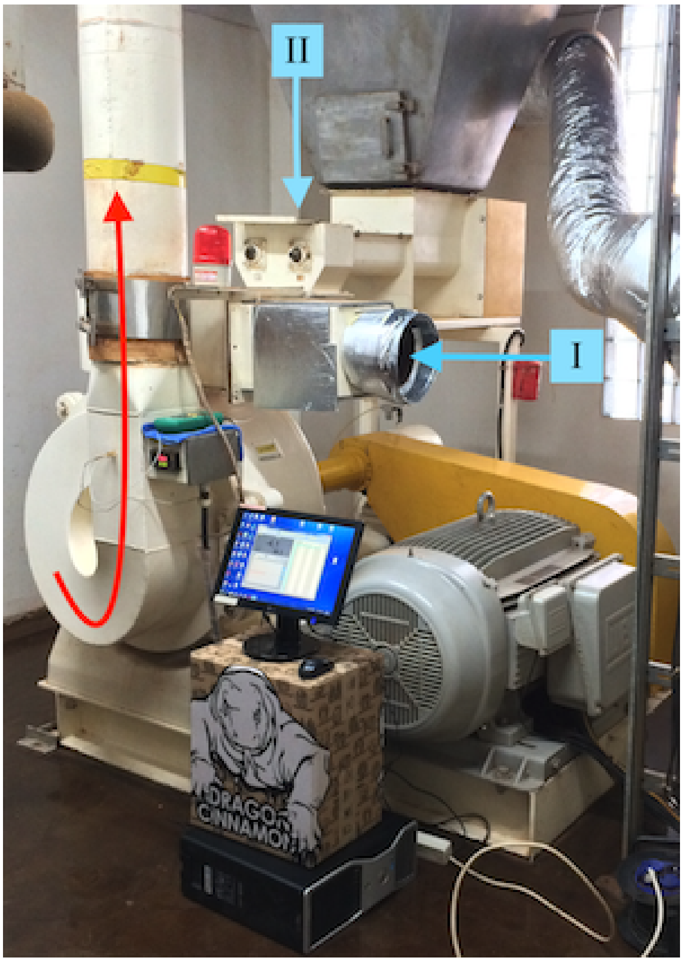

The standard layout for GRIN01.

D RSM experiments for settings under standard conditions

The measured loss responses for the determining the optimal settings of GRIN01 under standard conditions. Factor A is the feeder speed (RPM) and Factor B is the blade speed (RPM).

Experiment	Factor: A	Factor: B	Response: Loss (%)
1	30	1600	5.9
2	40	1600	6.1
3	30	1700	6.8
4	40	1700	7.6
5	28	1650	6.7
6	42	1650	7.1
7	35	1580	5.8
8	35	1720	7.0
9	35	1650	5.7
10	35	1650	5.9
11	35	1650	6.0
12	35	1650	5.7
13	35	1650	5.9

E Working principle inlet cooling system

The Water Chiller

One of the most commonly used cooling principles in industrial applications is The Vapour Compression Refrigeration Cycle. The cooling process takes place in a closed loop system where a refrigerant with a low boiling point goes through four basic steps to absorb/release heat: compression, condensation, expansion and evaporation, depicted in the figure below. In the first step, the refrigerant is compressed such that it will increase its temperature drastically. Then the hot compressed refrigerant is flown through a condenser which acts as a heat exchanger; the cool water from the cooling tower will absorb the relatively high temperature of the refrigerant, causing the refrigerant to (partly) condensate. The heated water will be cooled down by a cooling tower outside while the colder refrigerant is passed through an expansion valve inducing a sudden pressures drop. This pressure drop will drastically reduce the temperature of the refrigerant which will then go through the evaporator. The evaporator will again act as a heat exchanger, only this time its the refrigerant that absorbs the heat from the water coming from the AHU. The cooled water will be lead to the coils in the Air Handling Unit (AHU) to cool down the passing air, while the heated refrigerant will be compressed again (Moran et al., 2010).

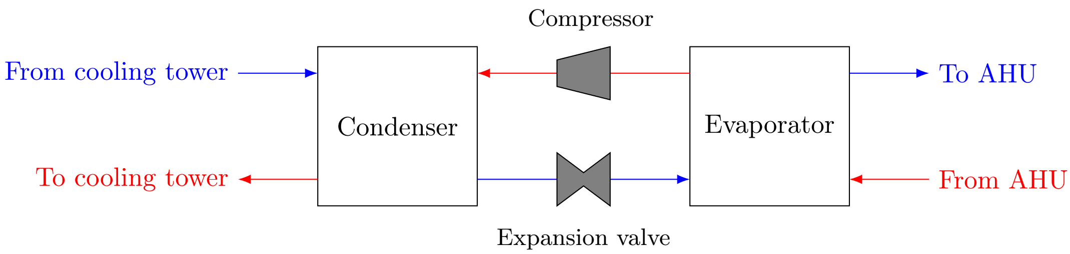

The vapour compression refrigeration cycle.

Note that the complete chiller system consists of the compression refrigeration cycle *and* integrated cooling tower.

The Air Handling Unit

The AHU regulates the air flow into the desired area, by sucking in and filtering the ambient air, after which it passes the coil evaporators. These coils are cooled down by the water coming from the evaporator of the water chiller, such that it absorbs the heat from the airflow that passes through the coils. The cooled down air then exits the AHU to go to the desired location (the grinder in this case).

F Inlet Cooling System installed on GRIN01.

The ducting coming from the AHU connected to the two air inlets (I & II) of GRIN01.

The (blue) AHU on the left, connected to GRIN01 through isolated ducting.

The chiller, placed outside, connected to the AHU through the tubes going into the wall.

G Costs for inlet cooling system

Rental Option

Except for the installation costs, the rental plan will have no further capital expenditures. According to the vendor, the expected lifetime of the chiller is estimated to be 5 years. Therefore, the depreciation period of the installation costs is also set at 5 years, since after this period a new (better) chiller might be available which needs to be installed. As for the operational costs, the management team of Tripper Nature said that no increase in manpower in necessary in order to operate the system. Therefore the increase in operational costs consists only of the monthly rent, the electricity bill and the replacement of air filters. As for the power usage, the vendor mentioned that the complete cooling system operates at 56 kW. The yearly operational hours of the cooling systems will be equal to the total operational hours of GRIN01 of 1,273 hours (1030 hours for DRAG60 and 243 hours for DRAG50), resulting in yearly energy usage of 71,288 kWh. The price per kWh in Indonesia is IDR 1,035 ($0.07), which results in yearly operational expenses of $4,990. The total yearly costs for using the inlet cooling system adds up to $16,642, which is equal to $13.07 per operational hour.

Overview of yearly additional costs for the rental option.

Expenditures	Type	Period	Costs	Yearly costs
Capital	Installation	5 years	$750	
				$150
Operational	Rent	1 month	$950	
	Electricity	1 year	$4,990	
	Air filters	6 months	$51	
				$16,492
			Total	$16,642

Buy Option

In the case of buying the complete cooling system, the capital expenditure rises, while the operational expenditure will decrease. For the capital expenditures, the initial investment for the chiller and the AHU will be added for $30,000.00 and $4,500.00 respectively. According to the vendor, the depreciation period for the chiller is at 5 years, while the period for the AHU is 10 years. The operational expenditures consist of again the electricity costs, the air filters with the addition of maintenance. After discussion with the vendor and management, the maintenance costs are estimated to be 10% of the initial price of the cooling system at $3,450.00.

Overview of yearly additional costs for the buy option.

Expenditures	Type	Period	Costs	Yearly costs
Capital	Installation	5 years	$750	
	Chiller	5 years	$30,000	
	AHU	10 years	$4,500	
				$7,200
Operational	Maintenance	1 year	$3,450	
	Electricity	1 year	$4,041	
	Air filters	6 months	$51	
				$ 8,542
			Total	$15,742

H RSM experiments on GRIN01 with inlet cooling

The measured loss responses for the different experiments to determine the optimal settings when using the inlet cooling system. Factor A is the feeder speed (RPM) and Factor B is the blade speed (RPM).

Experiment	Factor: A	Factor: B	Response: Loss (%)
1	30	1600	3.90
2	40	1600	4.70
3	30	1700	4.93
4	40	1700	5.20
5	28	1650	4.10
6	42	1650	5.56
7	35	1580	4.03
8	35	1720	5.42
9	35	1650	4.36
10	35	1650	4.48
11	35	1650	4.52
12	35	1650	4.12
13	35	1650	4.27

I Operational expenditures increase for pre-grind options

Since we are interested in the increase in costs for the pre-grind option, we will calculate the costs for regular DRAG60 and compare it to the costs for the pre-grind solution. The price per kWh in Indonesia is IDR 1,035 ($0.07), and the labour costs per hour for GRIN01 is $8.29 (Tripper Nature, 2018). The table below shows that the total yearly costs will increase by $9,260.

Overview of yearly additional costs for the pre-grind option.

Production type	Type	Production (h)	Costs	Total
Regular	Labour	1030	$8,538	
	Grinding (56 kW)	1030	$4,037	
				$12,576
Pre-grind	Labour	2060	$17,077	
	Pre-grind (36 kW)	1050	$2,595	
	Re-grind (30 kW)	1050	$2,163	
				$21,836
			Increase	$9,260